Text S1: Parametric uncertainty quantification

We gauged the level of uncertainty related to values of each parameter based on both literature and expert knowledge. For use of expert knowledge, we conducted workshops in 2008 and 2009 that included members of our own lab and two other mosquito ecology labs: Professor Thomas Scott's Lab (University of California, Davis) and Professor Laura Harrington's Lab (Cornell University). In the workshops, we explained the meaning of each parameter to the participants and we described to them our approach for visualizing and quantifying values of uncertainty (see Figure S1.1).

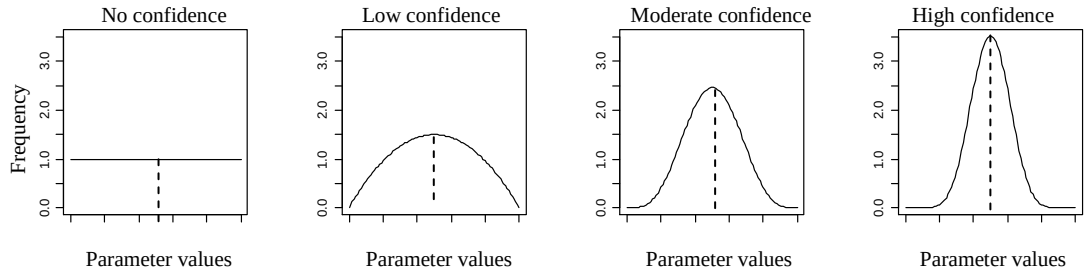

Figure S1.1 Probability distributions used to describe differing levels of uncertainty in the value of a parameter, x, whose default value is $x_{default}$ and for which the lower and upper limits are x_{min} and x_{max}. Uncertainty in the value of x is described by a beta distribution, with the scaled value $y = (x - x_{min})/(x_{max} - x_{min})$ following a beta distribution with parameters α and β. We take $\alpha = \gamma (x_{default} - x_{min})/(x_{max} - x_{min})$ and $\beta = \gamma (x_{max} - x_{default})/(x_{max} - x_{min})$. The parameter γ characterizes the confidence in the default value of the parameter, with $\gamma = 4$ if confidence is low, $\gamma = 10$ if confidence is moderate, and $\gamma = 20$ if confidence is high. For the examples shown, we have assumed that $x_{default}$ falls exactly halfway between the lower and upper limits, i.e. $x_{default} = (x_{min} + x_{max})/2$, giving symmetric distributions. In general, however, the distributions are asymmetric about $x_{default}$.

The participants were asked to provide, for each parameter, their expert opinion on the extreme possible values the parameter could take and their confidence in the default value of this parameter (the assumed most likely value based on data and experience), expressed as one of four levels of confidence: 1) no confidence; 2) low confidence; 3) moderate confidence; and 4) high confidence (see Figure S1.1). We emphasized to the participants that we wanted their answers to reflect, as much as possible, the views of the mosquito ecology research community. We then defined the range of possible values for each parameter based on the collected opinions on extreme values, and we used the expressed level of confidence to define the probability distribution of specific values within this range. If we had no confidence for a particular default value, then we assigned a uniform distribution to the probability distribution over the possible range. Otherwise, we used a beta distribution, scaled to the possible range, to assign higher probabilities to values near the default value, setting the likelihood of the default value in the low, moderate and high confidence scenarios to be approximately

1.5, 2.5 and 3.5 times as large as that defined in the uniform distribution (Figure S1.1). Generally, experts in the workshops agreed on the ranges and confidence levels in the default value for each parameter. When there was no consensus, we used the minimum value provided for the lower range and maximum value provided for the upper range. For the confidence levels in default values, we used the levels with majority agreements.

For parameters not directly measurable in the field or in the lab, it was difficult for the experts to provide their knowledge about the uncertainty. For most parameters, the literature provides both means (default values) and estimates of experimental uncertainty (e.g., standard errors). However, for parameters in the weight gain model and in the development rate model (see Text S2 and S3), where the original paper only reported the estimated values but no associated uncertainty, we digitized figures in the original paper and re-estimated the parameters to get their possible ranges and the confidence levels of default values (see Text S1.2 and S1.3).

S1.1. Uncertainty in survivorship

In Skeeter Buster, adult mosquito survivorship can either be assumed to be age-independent or age-dependent. In this uncertainty analysis, we assume that the survival rate is constant. Since the effect of age-dependent survival for female adults only becomes evident after about 20 days in laboratory experiments [1], this assumption should not have a major effect on the validity of our uncertainty analysis results given the shorter life-spans of mosquitoes in the field resulting from predation and other environmental factors. Based on our workshops and the literature [2,3,4,5,6], the default value for nominal survival rate for female adults and male adults is set at 0.89 and 0.77 respectively. Uncertainty in the nominal survival rate is assigned with a range from 0.75 to 0.99 and a range from 0.72 to 0.99 for female adults and male adults, respectively. Based on our workshops, we conclude that there is moderate confidence in the default values. It should be borne in mind, particularly when considering values at the upper ends of these ranges, that Skeeter Buster considers additional effects of temperature and moisture on mosquito survival. See Table S1, S2 and S3 for details on our use of categories of confidence and quantifications for survival parameters of adults, larvae, pupae and eggs.

S1.2. Uncertainty in weight gain model

Uncertainties in the parameters of larval weight gain model are defined based on a re-estimation of parameters using the larval weight data from Gilpin & McClelland [7] and a Metropolis-Hastings fitting algorithm [8,9] (see Text S2 for details). Based on the defined uncertainties in model parameters, for a 200ml cup with 40 mg liver powder and 20 larvae (initial weight = 0.001 mg), the 95% confidence interval for predicted weight after 4 days ranges between 0.28 and 0.62 mg (see Figure S1.2). Uncertainty in the predicted weight gain is relatively larger for larvae with higher body weights due to the propagation of uncertainty in the weight gain model.

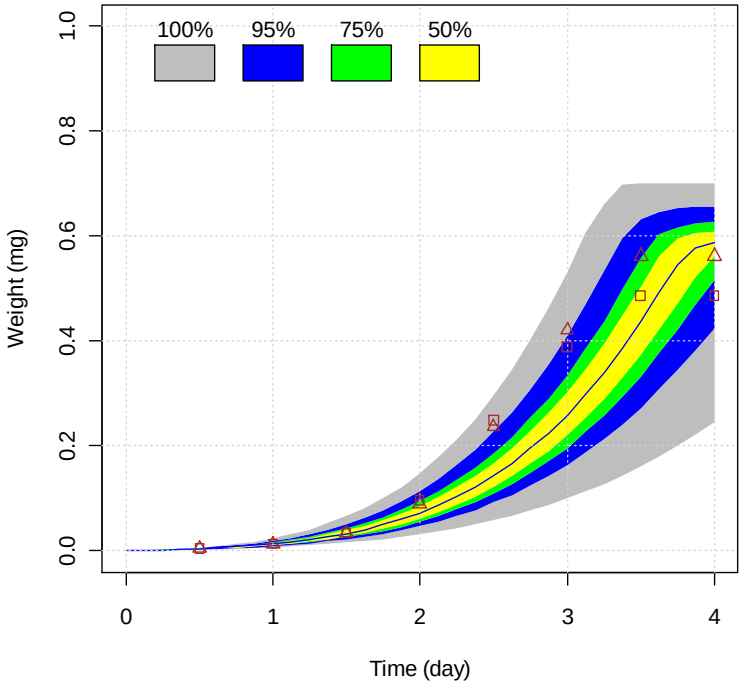

Figure S1.2 Uncertainty in the predicted larval weights by the weight gain model with parametric uncertainties defined in Table S4. Initially, 40 mg of food and 20 larvae are present. The yellow, green, blue and grey bands represent the 50% ,75% ,95% confidence interval of the prediction, respectively. The grey band represents the output boundary. The central blue line is the median. Symbols depict data points from Gilpin & McClelland [3] (squares: “house strain”, triangles: “bush strain”).

S1.3. Uncertainties in development times

Uncertainty in the estimation of development times was calculated based on a re-estimation of four parameters in a enzyme kinetics model [8, see eq. (S7)] using data from the literature (Tun-Lin et al. [9], Rueda et al. [10], Focks et al. [11] and Farnesi et al. [12]) and a Metropolis-Hastings fitting algorithm (see section S3 in Supplementary Materials). We used standard deviations of estimated development times from the literature to construct possible development time ranges at different temperatures. These ranges defined our uncertainty in the development rate response curve as a function of temperature. This uncertainty in the functional curve was of more interest to us than uncertainties in individual parameters of the enzyme kinetics model, since the parameters themselves have limited biological meaning [13]. Instead, the use of this model should be seen as a means to construct a non-linear relationship between development and temperature. The uncertainty in the estimated relationship between temperature and development rate itself was therefore more relevant than the uncertainties associated with each individual parameter.

We represented uncertainty in the response of development rate to temperature with an ensemble of 2000 development rate response curves generated by the Metropolis-Hastings method. A development rate response curve corresponds to a specific value of each of the four parameters in the enzyme kinetics model, and

defines the relationship between development rate and temperature. For the uncertainty analysis of the Skeeter Buster model, we draw random samples of development rate response curves from the ensemble (see Text S3 for details) to quantify the amount of uncertainty in model outputs contributed by uncertainty in the estimated relationship between temperature and development rate.

The resulting temperature-dependent uncertainties for development times for eggs, larvae, pupae and gonotrophic cycle durations are shown in Figure S1.3. We can see that uncertainty in development time is relatively high at lower temperatures, which is attributed to three reasons. First, lower temperatures lengthen the time taken to complete the life stage, which gives a higher potential for individual variability to accumulate. Second, the lower survival rate due to very low temperature will result in a reduced number of individuals completing the specific stage, with the resulting smaller sample size leading to lower confidence for the estimated development time. Third, the model structure itself may not be able to capture the development time at extreme environmental conditions. This is one type of structural uncertainty. The large uncertainty at lower temperatures may play a large role in temperate areas, but may not have much effect on model predictions for our study area since the temperature there is generally higher than 20 ^{o}C (see Figure S3).

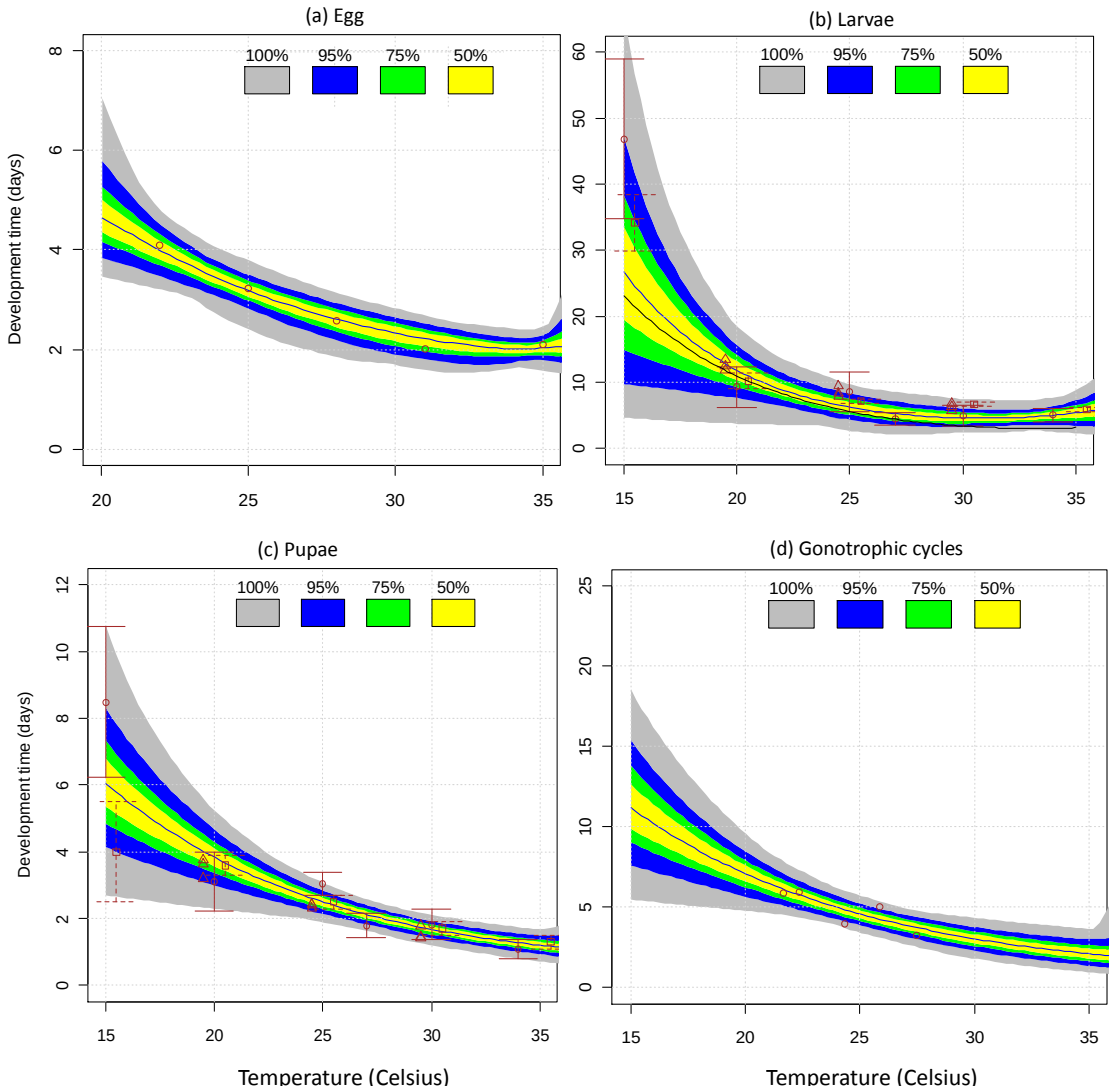

Figure S 1.3 Uncertainty in the estimation of development times for (a) eggs, (b) larvae, (c) pupae and (d) gonotrophic cycle duration as functions of temperature. The embryonic development times for eggs are estimated based on data from Farnesi et al. [12]. The development times for larvae and pupae are estimated based on data from Rueda et al. [10] and Tun-Lin et al. [9]. The estimated uncertainty encompasses data from Kamimura et al. [14]. In panels (b) and (c), the circles represent data from Rueda et al. [10] and the squares (shifted to the right by 0.5 ºC to aid visibility) are data from Tun-Lin et al. [9]. The triangle points (shifted to the left by 0.5 ºC to aid visibility) represent the data from Kamimura et al.[14]. The gonotrophic cycle durations are estimated based on data from Focks et al [11]. The vertical lines indicate the standard deviations (+/- one standard deviation) of the development times. The central line represents the median of the prediction based on the parameter sets sampled by FAST. The yellow, green, blue and grey bands represent the 50% ,75% ,95% confidence interval of the prediction, respectively. The grey band represents the output boundary.

S1.4. Uncertainty in spatial dispersal

There is a large amount of uncertainty in the estimate of *Ae. aegypti* dispersal [see 15, Chapter 15 for a review]. The maximum dispersal distance ranges from 100 to 800 meters. The spatial dispersal rate is mainly estimated based on the mark-release-recapture approach and the associated uncertainty is assumed to result from different factors including sampling error, recapture rate, mosquito survival, breeding site availability, and environmental heterogeneity. In the Skeeter Buster model, two types of dispersal are used to model mosquito movement: short-range dispersal (dispersal to a neighboring house), and long-range dispersal (dispersal from the original house to any other within a specified maximum dispersal distance). Harrington et al. [16] showed that, in their mark-release-recapture experiments, the majority of mosquitoes (72% of males and 65% of females) were captured in houses adjacent to their outdoor release location during 4-12 capture days. Thus, our assumption in the Skeeter Buster model that short-range dispersal between neighboring houses is the major dispersal mechanism is consistent with these observations. An adult mosquito may, however, make short-range dispersals on more than one day, so its lifetime dispersal could cover several houses [17]. The uncertainty range of daily probability of short-range dispersal is defined between 0.05 to 0.5 with a default value of 0.3, which is fitted using Harrington's data [16,17]. The daily probability of long-range dispersal is defined between 0 and 0.1 with a default value of 0.02. The confidence for default values of both female and male adults is defined to be low based both on the literature and expert opinion. See Table S5 for details of uncertainty quantifications for all spatial dispersal parameters.

S1.5. Correlation among model parameters

Model parameters are often assumed to be independent. However, they may be correlated as a result of common factors (e.g., common environmental factors or factors controlling the different biological parameters). For example, if a specific environmental factor favors survival of female adults, it is highly likely that the survival of male adults will also be favored. This can lead to a correlation between survival rates of male adults and those of female adults. However, if we assume independence of parameters, the sampling of parameters undertaken as part of the uncertainty analysis could generate unrealistic combinations (e.g., the survival rate for male adults is very high while the survival rate for female adults is very low). Thus, it is important to incorporate potential correlations among parameters. In uncertainty analysis, taking correlation into account for linear models (i.e., the model outputs are linearly dependent on model parameters) can often increase the amount of uncertainty in the model's predictions if positive correlation is assumed (due to the enhanced population dynamics if sampled values of two parameters are both high, assuming parameters are positively correlated with model output) and decrease the amount of uncertainty in the model's predictions if negative correlation is assumed (due to the balancing of population dynamics by low and high parameter values, assuming parameters are positively correlated with model output). However, for complex models, the effects of correlation on uncertainty can be different due to the complex

relationships (e.g., nonlinear and non-monotonic relationships) between model predictions and individual parameters.

For most of the parameters, it is difficult to estimate the correlations among them based on available data, thus the correlation values are simply a best estimate from expert opinion. In this study, we assume a rank correlation of 0.3 between nominal survival rates for female and male adults, between nominal survival rates for larvae and pupae, between the survival factor under high sun exposure and that under high saturation deficit, between the short-range dispersal probabilities for females and males, and also between long-range dispersal probabilities for females and males. A correlation coefficient of 0.89 is assigned between intercept and slope for lipid prediction (see eq. (S2.6) in Text S2), which is based on the data fitting using a linear regression. All other parameter combinations are considered as being independent of each other because we lack information that clearly suggests that a correlation exists.

References:

1. Styer LM, Carey JR, Wang JL, Scott TW (2007) Mosquitoes do senesce: Departure from the paradigm of constant mortality. Am J Trop Med Hyg 76: 111-117.
2. Maciel-De-Freitas R, Codego CT, Lourenco-De-Oliveira R (2007) Body size-associated survival and dispersal rates of *Aedes aegypti* in Rio de Janeiro. Med Vet Entomol 21: 284-292.
3. Harrington LC, Edman JD, Scott TW (2001) Why do female *Aedes aegypti* (Diptera: Culicidae) feed preferentially and frequently on human blood? J Med Entomol 38: 411-422.
4. Harrington LC, Vermeylen F, Jones JJ, Kitthawee S, Sithiprasasna R, et al. (2008) Age-dependent survival of the dengue vector *Aedes aegypti* (Diptera : Culicidae) demonstrated by simultaneous release-recapture of different age cohorts. J Med Entomol 45: 307-313.
5. McDonald PT (1977) Population characteristics of domestic *Aedes aegypti* (Diptera: Culicidae) in villages on Kenya coast. 1. Adult survival and population size. J Med Entomol 14: 42-48.
6. Sheppard PM, Macdonal.Ww, Tonn RJ, Grab B (1969) Dynamics of an adult population of *Aedes aegypti* in relation to dengue haemorrhagic fever in Bangkok. J Anim Ecol 38: 661-702.
7. Gilpin ME, McClelland GAH (1979) Systems-analysis of the yellow fever mosquito *Aedes aegypti*. Forts Zool 25: 355-388.
8. Sharpe PJH, DeMichele DW (1977) Reaction kinetics of poikilotherm development. J Theor Biol 64: 649-670.
9. Tun-Lin W, Burkot TR, Kay BH (2000) Effects of temperature and larval diet on development rates and survival of the dengue vector *Aedes aegypti* in north Queensland, Australia. Med Vet Entomol 14: 31-37.
10. Rueda LM, Patel KJ, Axtell RC, Stinner RE (1990) Temperature-dependent development and survival rates of *Culex quinquefasciatus* and *Aedes aegypti* (Diptera: Culicidae). J Med Entomol 27: 892-898.
11. Focks DA, Haile DG, Daniels E, Mount GA (1993) Dynamic life table model of *Aedes aegypti* (Diptera: Culicidae) - Analysis of the literature and model development. J Med Entomol 30: 1003-1017.
12. Farnesi LC, Martins AJ, Valle D, Rezende GL (2009) Embryonic development of *Aedes aegypti* (Diptera: Culicidae): influence of different constant temperatures. Mem Inst Oswaldo Cruz 104: 124-126.
13. Otero M, Schweigmann N, Solari HG (2008) A stochastic spatial dynamical model for *Aedes aegypti*. Bull Math Biol 70: 1297-1325.
14. Kamimura K, Matsuse IT, Takahashi H, Komuka J, Fukuda T, et al. (2002) Effect of temperature on the development of *Aedes aegypti* and *Aedes albopictus*. Med Entomol Zool 53: 53-58.
15. Silver JB (2008) Mosquito Ecology. New York, USA: Springer. 1477 p.
16. Harrington LC, Scott TW, Lerdthusnee K, Coleman RC, Costero A, et al. (2005)

Dispersal of the dengue vector *Aedes aegypti* within and between rural communities. Am J Trop Med Hyg 72: 209-220.

17. Magori K, Legros M, Puente ME, Focks DA, Scott TW, et al. (2009) Skeeter Buster: a stochastic, spatially-explicit modeling tool for studying *Aedes aegypti* population replacement and population suppression strategies. Plos Neglect Trop Dis 3: e508.

Text S2: Parameter estimation for the larval weight gain model

The larval weight gain model [1] is governed by two equations:

$$\begin{aligned} \frac{dW(t)}{dt} &= aW(t)^b(1-e^{-cF(t)}) \\ \frac{dF(t)}{dt} &= -\frac{1}{a}N(t)\frac{dW(t)}{dt} \end{aligned} \qquad \text{(S2.1)}$$

where $N(t)$ is the total number of larvae in the container, $W(t)$ is the larval weight (mg), and $F(t)$ is the amount of food (mg) in the container at time *t*. The factor a is the conversion rate of consumed food to biomass, *b* represents the body weight effect on larval food exploitation rate, and *c* is the coefficient of food dependence, with a lower value indicating a stronger effect of food on larval growth (see Figure S2.1 for more explanations) and a stronger effect of density dependence on larval population growth.

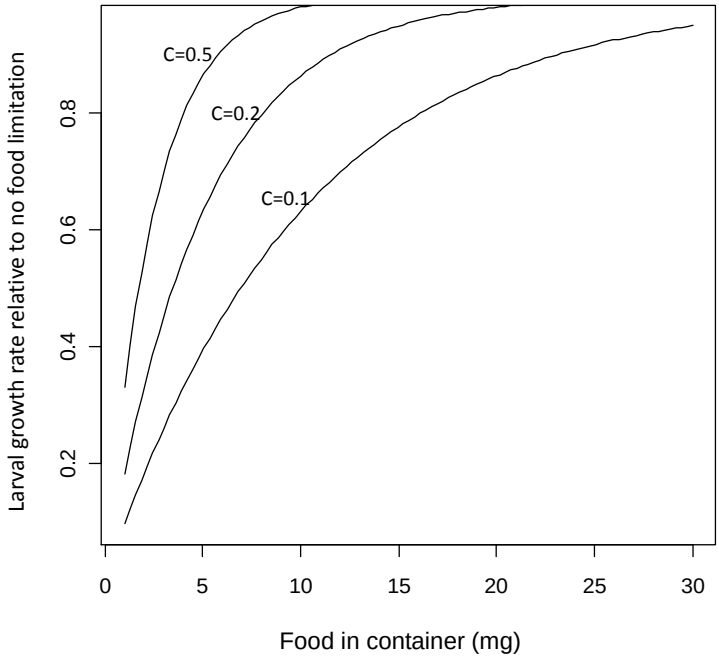

Figure S2.1 Effect of the food amount in water containers on larval growth with different coefficients of food dependence based on the larval weigh gain model as specified in eq.(S2.1). A lower value of the coefficient of food dependence leads to a stronger effect of food on larval growth.

In order to estimate the three model parameters in eq. (S2.1), we assume that the

observed data can be described by log-normal distributions as follows

$$\log w(t) \sim N(\log w(t)_p, \sigma^2). \qquad \text{(S2. 2)}$$

In other words, the logged larval weight is normally distributed with mean [i.e., $\log w(t)_p$] predicted by the larval weight gain model and variance σ^2. The experiment use three different levels food inputs (0.25 g, 0.1 g and 0.04 g liver powder in a 200 ml cup), four levels of larvae inputs (8, 20, 51 and 128), two strains (house and bush strain). With weight sampling at 12 hour intervals, there are 160 weight observation data points. Observations made at the first time point for each experiment are taken as initial values for the weight gain model in eq. (S2.1).

We employ a Bayesian approach to estimate model parameters. The prior distributions for the parameters are specified as follows,

$$\begin{aligned} a &\sim \text{Uniform}[0, 0.5] \\ b &\sim \text{Uniform}[0,1] \\ c &\sim \text{Uniform}[0,1] \\ \frac{1}{\sigma^2} &\sim \text{Gamma}(0.001, 0.001) \end{aligned} \qquad \text{(S2.3)}$$

where Uniform[α, β] represents a uniform distribution with on the interval [α, β]; Gamma (α, β) represents a gamma distribution. With the specified prior distribution for parameters and the statistical model for data specified in eq.(S2.2), Bayes' rule is used to derive the posterior distribution for the parameters given the observed data as follows,

$$\begin{aligned} & f(a,b,c,\sigma^2 \mid w_1,....,w_n) \\ & \propto f(w_1,....,w_n \mid a,b,c,\sigma^2) f(a) f(b) f(c) f(\sigma^2) \qquad \text{(S2.4)} \\ & = (\frac{1}{\sqrt{2\pi\sigma^2}})^n \exp[-\frac{1}{2\sigma^2}\sum_{i=1}^{n}(\log w_i - \log w_{ip})^2] f(a) f(b) f(c) f(\sigma^2) \end{aligned}$$

where $w_1,....,w_n$ are the observed body weights and w_{ip} are the predicted larval weights. The function $f(a), f(b), f(c), \text{and } f(\sigma^2)$ are the prior probability distribution functions defined in eq. (S2.3). Since the posterior distribution in eq. (S2.4) can be very difficult to derive analytically, in this study, the Metropolis-Hastings approach [2,3] is used to draw samples for the parameters from the posterior distribution. Specifically, the algorithm is implemented as follows,

1) Assign initial values to a,b,c,σ^2;
2) Run the weight gain model in eq. (S2.1), which is numerically evaluated using the Euler method;
3) Calculate the posterior likelihood $f(a,b,c,\sigma^2 \mid w_1,....,w_n)$ based on eq. (S2.4);

4) Propose new values for parameters with a multivariate normal distribution

$a = a^*, b = b^*, c = c^*, \sigma^2 = \sigma^{2*}$;

5) Calculate the posterior likelihood $f(a^*, b^*, c^*, \sigma^{2*} \mid w_1, ..., w_n)$ based on eq. (S2.4);

6) Draw a random sample u from uniform [0,1]. If

$$u < \frac{f(a^*, b^*, c^*, \sigma^{2*} \mid w_1, ..., w_n)}{f(a, b, c, \sigma^2 \mid w_1, ..., w_n)},$$

then accept the new proposed parameter values; otherwise stay put.

7) Repeat step 4)-6).

It can be shown that sample drawn by the Metropolis-Hastings method will follow the posterior distribution using the fact that the Markov chain is stationary if the proposal distribution is symmetric [4].

In this study, we run a chain of 150,000 iterations and a burn size of 50, 000 (the initial sequence of samples that is discarded to eliminate dependence on the initial choice of parameter values). We calculate the statistics of estimated parameters using every tenth sample of the parameters (to reduce the effect of auto-correlation on sample statistics) (See Table S2.1).

Table S2.1 Estimated parameters for the weight gain model

	a	b	c	σ^2
mean	0.32	0.80	0.55	20.07
Standard deviation	0.0077	0.0060	0.25	2.25

The weight gain model in eq.(S2.1) specifies the net growth of larval weight. A full version of the weight gain model has an additional term for metabolic weight loss as follows,

$$\frac{dW(t)}{dt} = a\,[W(t)^b(1 - e^{-cF(t)}) - d_1 W(t)^{d_2}] \qquad \text{(S2.5)}$$

where $d_1 W(t)^{d_2}$ represents biomass loss due to metabolic activity. d_1 is the coefficient of metabolic weight loss, with a higher value indicating higher amount of energy is used for metabolic activity, and d_2 represents the effect of body weight on metabolic activity and is commonly set at 2/3 [5]. Since the metabolic weight loss term in the larval weight gain model (i.e., $d_1 W(t)^{d_2}$) is not identifiable based on the available data, the coefficient of metabolic weight loss (i.e., d_1) was assigned with a range between 0.005 and 0.032 based on expert opinion. This means that the percent of weight loss by metabolic activities is between 0.5 and 3.2 percent of body weight gain with no food constraint.

If there is no food available in the container, then the amount of lipid reserve in larva's body can be crucial for survival. In Skeeter Buster, the amount of lipid is

calculated using the following linear function of the logged larval weight, obtained by applying linear regression to data from Gilpin and McClelland [5],

$$L(t) = L_a \ln W(t) + L_b, \qquad \text{(S2.6)}$$

where $L(t)$ is the percentage of lipid weight in the larva's body at time t. The L_a and L_b are the slope and intercept, respectively. The mean and standard deviations of L_a and L_b (see Table S4) are estimated based on fitting of the linear regression to the data from Gilpin and McClelland [5].

References:

1. Gilpin ME, McClelland GAH (1979) Systems-analysis of the yellow fever mosquito *Aedes aegypti*. Forts Zool 25: 355-388.
2. Metropolis N, Rosenbluth AW, Rosenbluth MN, Teller AH, Teller E (1953) Equation of state calculations by fast computing machines. J Chem Phys 21: 1087-1092.
3. Hastings WK (1970) Monte Carlo sampling methods using Markov chains and their applications. Biometrika 57: 97-109.
4. Gelman A (2004) Bayesian data analysis. Boca Raton, Fla.: Chapman & Hall/CRC. xxv, 668 p. p.
5. Gilpin ME, McClelland GAH (1979) Systems-analysis of the yellow fever mosquito *Aedes aegypti*. Forts Zool 25: 355-388.

Text S3: Parameter estimation for the enzyme kinetics model

The developmental rates of different life stages in the Skeeter Buster model are simulated based on an existing enzyme kinetics model [1]. This enzyme kinetics model assumes that development rate is determined by a single rate-controlling enzyme and that the enzyme is denatured at high and low temperatures. A simplified version of this model [2] is used in the Skeeter Buster model, assuming inactivation only at high temperatures. The developmental rate is calculated based on a nonlinear equation with four parameters,

$$r(T_t) = \frac{\rho_{(25^\circ\mathrm{C})} \frac{T_t}{298} e^{\frac{\Delta H_A^{\neq}}{R}(\frac{1}{298} - \frac{1}{T_t})}}{1 + e^{\frac{\Delta H_H}{R}(\frac{1}{T_{1/2H}} - \frac{1}{T_t})}}, \qquad \text{(S3.1)}$$

where $r(T_t)$ is the developmental rate (hr^{-1}) at temperature T (K) on day t, T_t is the water temperature for all immature stages and air temperature for adults. $\rho(25^oC)$ is the development rate (hr^{-1}) at 25ºC assuming no temperature inactivation of the critical enzyme; $\Delta H_A^{\neq}$ is the enthalpy of activation of the reaction catalyzed by the enzyme (cal/mol); ΔH_H is the enthalpy change associated with high temperature inactivation of the enzyme (cal/mol); and $T_{1/2H}$ (K) is the temperature at which 50% of the enzyme is inactivated from high temperature.

In order to estimate the model parameters (T_t , $\rho(25^oC)$, $T_{1/2H}$ and $\Delta H_A^{\neq}$), we assume the observed data follow normal distributions as follows

$$D(T) \sim N(D(T)_p, \sigma^2(T)) \qquad \text{(S3.2)}$$

where $D(T)_p$ is the predicted development time at temperature T using eq. (S3.1) and $\sigma^2(T)$ is the standard deviation of the observed development times at temperature T.

We use development time data at different temperatures from Farnesi et al.[3] to estimate the embryonic development rate (see Figure S1.3 in Text S1). Since the standard deviation for mean development time is very low due to the well-controlled laboratory conditions of the experiment, we increase the standard error proportionally based on data utilized by Focks et al. [4] to estimate egg development time to reflect the view that the field environment can cause higher variability in development times. The development times for larvae and pupae are estimated based on data from Rueda et al [5] and Tun-Lin et al [6]. The means and standard errors at different temperatures are weighted for different data sources with the weights chosen to be proportional to the sample sizes. The development times of gonotrophic cycles are estimated using data from Focks et al [4].

We employ a Bayesian approach to estimate model parameters. The prior distributions for parameters are specified as follows,

$$
\begin{aligned}
&T_t \sim \text{Uniform } [300, 330] \\
&\rho_{(25^{o}\text{C})} \sim \text{Uniform } [0,1] \\
&\Delta H_{\text{A}}^{\neq} \sim \text{Uniform } [1000, 200000] \\
&\Delta H_{\text{H}} \sim \text{Uniform } [1000, 200000].
\end{aligned}
\tag{S3.3}
$$

Based on the specified prior distribution for model parameters and the statistical model for data in eq. (S3.2), Bayes' rule is used to derive the posterior distribution for the parameters given the data as follows,

$$
\begin{aligned}
&f(T_t\ ,\ \rho_{(25^{o}\text{C})},\ \Delta H_{\text{A}}^{\neq},\ \Delta H_{\text{H}} \mid D_1, ..., D_n) \\
&\propto f(T_t\ ,\ \rho_{(25^{o}\text{C})},\ \Delta H_{\text{A}}^{\neq}, \Delta H_{\text{H}} \mid a, b, c, \sigma^2)\, f(T_t)\, f(\rho_{(25^{o}\text{C})})\, f(\Delta H_{\text{A}}^{\neq})\, f(\Delta H_{\text{H}}) \\
&= \left(\frac{1}{\sqrt{2\pi\sigma_i^{\,2}}}\right)^n \exp\left[-\frac{1}{2\sigma_i^{\,2}} \sum_{i=1}^{n} (D_i - D_{ip})^2\right] f(T_t)\, f(\rho_{(25^{o}\text{C})})\, f(\Delta H_{\text{A}}^{\neq})\, f(\Delta H_{\text{H}})
\end{aligned}
\tag{S3.4}
$$

where $D_1, ..., D_n$ and $\sigma_1, ..., \sigma_n$ are the mean and standard deviations of observed development times at different temperatures. $f(T_t)$, $f(\rho_{(25^{o}\text{C})})$, $f(\Delta H_{\text{A}}^{\neq})$, and $f(\Delta H_{\text{H}})$ are the prior distribution function as defined in eq. (S3.3). Similar to the estimation of growth model parameters, the Metropolis-Hastings approach is used to draw samples for parameters in the enzyme kinetics model from the posterior distribution in eq. (S3.4). In this study, we run a chain of 150,000 iterations and a burn size of 50, 000. The estimated statistics for the posterior distribution (sampled every 50 steps on the Markov chain sequence) are shown in Table 3.1.

Table S3.1 Estimated parameters for development times of different life stages obtained using the Bayesian approach described in the text (Values in parentheses are standard errors).

Life Stages	*Parameters*			
	ρ(25ºC)	$\Delta H_{\text{A}}^{\neq}$	$T_{1/2\text{H}}$	ΔH_{H}
Eggs	0.34	14265	312.17	88762
	(0.06)	(5518)	(6.73)	(55073)
Larvae	0.201	26372	305.61	55648
	(0.049)	(9540)	(6.71)	(18910)
Pupae	0.483	15497	316.91	40605
	(0.121)	(3427)	(7.90)	(29622)
Gonotrophic	0.233	15106	319	100375
cycles	(0.044)	(3513)	(6.87)	(59600)

Since we are more concerned with the overall contributions to variances of model outputs by the uncertainties in development rates as a functional curve (or a profile) of temperature rather than the contribution by individual parameters**,** we used a

profile-based sampling approach to sample the development rate profiles. The main idea of the profile-based sampling is that, we use the mean development time under the temperature range between 24-28^{o}C, which is the most relevant ranges in our study area, to draw random samples of development-rate profiles. Each development-rate profile will correspond to a mean development time (Figure S3.1). For the uncertainty analysis, instead of drawing samples for the parameters, we draw a sample for the mean development time between 24-28^{o}C. For each mean development time drawn, we get corresponding parameter values for the enzyme kinetics model using a pool of 2000 development rate profiles (each with a specific set of parameter values) generated by the Metropolis-Hastings approach.

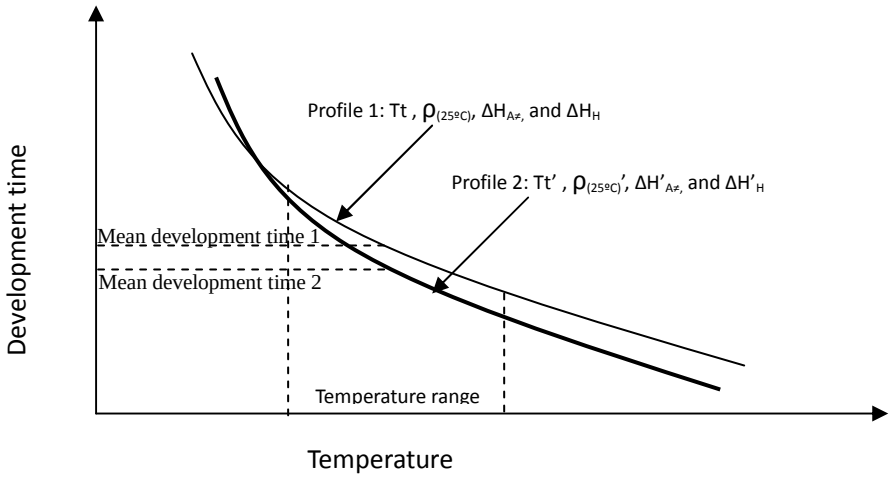

Figure S3.1 Illustration of mean development time within a specified temperature range as a surrogate for sampling of development time profiles. Development time profiles are profiles (or curves) assigning development rates under different temperatures, determined by an enzyme kinetics model in eq.(S3.1). Profile 1 and 2, both with a unique set of parameters (T_t , $\rho_{(25^{o}C)}$, $\Delta H_{A\neq}$ and ΔH_H), are represented by the mean development time within the specified temperature range (24-28^{o}C in this study). Each profile in a 2000 profile pool generated by a Metropolis-Hastings algorithm corresponds to a mean development time within the specified temperature range. For each sampled value of mean development time, a corresponding development profile in the pool with the same (or closest) mean development time will be selected to predict the development rate at different temperatures.

References:

1. Sharpe PJH, DeMichele DW (1977) Reaction kinetics of poikilotherm development. J Theor Biol 64: 649-670.
2. Schoolfield RM, Sharpe PJH, Magnuson CE (1981) Non-linear regression of biological temperature-dependent rate models based on absolute reaction-rate theory. J Theor Biol 88: 719-731.
3. Farnesi LC, Martins AJ, Valle D, Rezende GL (2009) Embryonic development of

Aedes aegypti (Diptera: Culicidae): influence of different constant temperatures. Mem Inst Oswaldo Cruz 104: 124-126.

4. Focks DA, Haile DG, Daniels E, Mount GA (1993) Dynamic life table model of *Aedes aegypti* (Diptera: Culicidae) - Analysis of the literature and model development. J Med Entomol 30: 1003-1017.
5. Rueda LM, Patel KJ, Axtell RC, Stinner RE (1990) Temperature-dependent development and survival rates of *Culex quinquefasciatus* and *Aedes aegypti* (Diptera: Culicidae). J Med Entomol 27: 892-898.
6. Tun-Lin W, Burkot TR, Kay BH (2000) Effects of temperature and larval diet on development rates and survival of the dengue vector *Aedes aegypti* in north Queensland, Australia. Med Vet Entomol 14: 31-37.

Text S4: Quantification of stochastic uncertainty

The predicted population density (for either a specific house or at the community level) for a given life stage *i* at time *t*, denoted $N_i(t)$, depends both on the parameter values of the model and on random noise (arising from demographic and environmental stochasticity). We can write

$$\mathrm{N}_i(t) = u_i(t) + e_i(t)$$

where $u_i(t)$ is the mean population size and $e_i(t)$ is the random noise. If we have two realizations of the model carried out using the same parameter values, then

$$\mathrm{N}'_i(t) - \mathrm{N}_i(t) = e_i(t) - e_i'(t).$$

Calculating the variance of both sides of the above equation, we can show that

$$Var[\mathrm{e}_i(t)] = \mathrm{Var}[\mathrm{N}'_i(t) - \mathrm{N}_i(t)] / 2.$$

This indicates that we can estimate stochastic uncertainty by running the model twice for each parameter set sampled by FAST. Namely,

$$\hat{Var}[\mathrm{e}_i(t)] = \frac{1}{2n}\sum_{i=1}^{n}[\mathrm{D}_{\mathrm{N}_i}{}^{(\mathrm{j})}(t) - \bar{\mathrm{D}}_{\mathrm{N}_i}{}^{(\mathrm{j})}(t)]^2$$

where $\mathrm{D}_{\mathrm{N}_i}{}^{(\mathrm{j})}(t)$ indicates the difference between two replicates for the *j*th FAST sample [$\mathrm{D}_{\mathrm{N}_i}{}^{(\mathrm{j})}(t) = \mathrm{N}'_i(t) - \mathrm{N}_i(t)$]; and *n* is the FAST sample size (5000 in our study). Finally, we can use the ratio of $\hat{Var}[\mathrm{e}_i(t)]$ to the total variance of $\mathrm{N}_i(t)$ to measure the proportion of stochastic uncertainty in the population density prediction at the community or individual-house level.

Text S5: Spatial statistics

In this study, we use three spatial statistics (Moran's *I*, Getis G_i^* (*d*) and semivariogram) to measure population distribution pattern. The Moran's Index, *I*, was proposed by Moran in 1950 to evaluate whether a spatial pattern is clustered, dispersed, or random [1]. A Moran's Index value near +1.0 indicates clustering, an index value near -1.0 indicates dispersion, and an index of 0 indicates complete randomness. The specific formula for calculating the Moran's *I* is as follows,

$$I = \frac{N}{\sum_i \sum_j w_{i,j}} \frac{\sum_i \sum_j w_{i,j}(x_i - \bar{x})(x_j - \bar{x})}{\sum_i (x_i - \bar{x})^2}$$

where *N* equals the number of observations; w_{ij} is the weight between locations *i* and *j*; x_i and x_j are the values at locations *i* and *j*; $\bar{x}$ is the average over all locations of the variable. In this study, the weight w_{ij} is proportion to the inverse distance between houses.

The Getis $G_i^*(d)$ statistic is used in this study to identify hot spots for food inputs at individual houses. The formula for $G_i^*(d)$ is as follows [2,3],

$$G_i^*(d) = \frac{\sum_{j=1}^{N} w_{ij}(d)x_j - \bar{x}\sum_{j=1}^{N} w_{ij}(d)x_j}{S\sqrt{[N\sum_{j=1}^{N} w_{ij}^2(d) - (\sum_{j=1}^{N} w_{ij}(d))^2]/(N-1)}}$$

where $w_{ij}(d)$ is the weight between locations *i* and *j* with a specified threshold distance *d*, which is used to specify the neighborhood size around of the house of interest to examine if this house is a local high/low density spot; and S is the standard deviation of all observations. In this study, we select $w_{ij}(d)$ based on the inverse distance throughout the study area (i.e., *d* is sufficiently big to incorporate all houses), which is same as that in the calculation of Moran's *I*. $G_i^*(d)$ has an asymptotic normal distribution. A *z*-score can be calculated to see if the population within a specific house is significantly higher/lower than its neighborhood.

The semivariogram is a function of distance describing the degree of spatial dependence of a spatial random process [4]. The formula is as follows,

$$r(h) = \frac{1}{|N(h)|} \sum_{i,j \in N(h)}^{N} |x_i - x_j|^2$$

where $N(h)$ is the set of data point pairs (x_i, x_j) that are distance *h* apart and $|N(h)|$ represents the number of data point pairs. A higher value of $r(h)$ indicates lower spatial autocorrelation. Generally, the spatial auto-correlation will decrease with distance *h* and finally stabilize. The range (i.e., the distance after which $r(h)$ starts to stabilize) can be used to indicate the strength of spatial auto-correlation.

References:

1. Moran PAP (1950) Notes on continuous stochastic phenomena. Biometrika 37: 17-23.
2. Getis A, Ord JK (1992) The analysis of spatial association by use of distance statistics. Geogr Anal 24: 189-206.
3. Ord JK, Getis A (1995) Local spatial autocorrelation statistics - distributional issues and an application. Geogr Anal 27: 286-306.
4. Goovaerts P (1997) Geostatistics for natural resources evaluation. New York: Oxford University Press. 483 p.

Text S6: Temporal variability of population density at the community level

In this section, we examine temporal variability in population density at the community level. Specifically, we assess contributions by different model parameters to uncertainty in the predicted temporal coefficient of variation (CV). The temporal coefficient of variation is calculated as follows: for each simulation run, we consider the community-level daily population densities seen over the second simulation year, calculating the standard deviation and mean of these densities. The CV is then calculated as the ratio of these two quantities. The temporal CV measures the relative temporal variability adjusted by population size. Temporal variability may result from stochastic uncertainty, biological development cycles, environmental factors (e.g., extreme temperature) and temporal dynamics of food. Since stochastic uncertainty is a major source of temporal variation, model parameters explain much less of uncertainties in temporal CV (generally less than 30% in total, see Figure S6.1 and S6.2) compared to population densities at the community level (see result section in the main text). For the egg density, the nominal survival rate for female adults and the gonotrophic development rate are two important parameters contributing to its temporal variability (Figure S6.1 a). The survival rate becomes an important parameter because it is a major factor affecting population size (see result section in the main text for details), which will affect the population's susceptibility to stochasticity. Parameters important for temporal variability in predicted larval population density include the high temperature limit for nominal egg survival, the high temperature limit for predator activities, as well as the nominal survival rate for female adults (Figure S6.1 b). The high temperature limits are important for temporal variability in the predicted larval population density because the maximum water temperatures on some days can reach (see Figure S3 c) the high temperature limits for nominal egg survival (defined as being between 28^{o}C to 35 ^{o}C) and high temperature limits for predator activities (defined as being between 25^{o}C to 35 ^{o}C). Important parameters contributing to temporal variability in the predicted pupal population density include the survival rate for female adults, the low temperature limit for nominal survival of pupae/larvae, the pupal development rate, and the coefficient of food dependence (Figure S6.1 c). The low temperature limit for survival of larvae/pupae is important because the minimum water temperatures are partially covered by this low temperature limit with its uncertainty range defined between 10^{o}C to 20 ^{o}C (see Figure S3 b). The coefficient of food dependence is important because it will affect the food exploitation rate, which can affect the temporal dynamics of food in the containers and the strength of density-dependence effect on larval growth. Strong density dependence in larval growth as determined by a small value of the coefficient of food dependence will lead to more temporal variability in population dynamics (see Figure S6.3). However, when the coefficient of food dependence is larger than 0.4, it tends to have much a less effect on temporal variability in population dynamics. This is because density dependence in larval growth become weak and food will only have effects on body growth when the food in container is very low (see Figure S2.1 in Text S2 for a better understanding).

For nulliparous female adults, the low temperature limit for nominal survival of pupae and larvae, and the survival rate of female adults are important parameters contributing to its temporal variability (Figure S6.2 a). Because the population dynamics of parous female adults is mainly affected by their survival rate (see result section in main text), the survival rate is also a dominant factor affecting the temporal variability (Figure S6.2 b), due to the fact that the population size can

affect the population's susceptibility to stochasticity (see result section in the main text for details). Other important parameters contributing to the temporal variability in predicted parous female adult density include the gonotrophic development rate, the nominal survival rate for male adults, and the low temperature limit for nominal survival of larvae/pupae. For temporal variability of male adults, important parameters include the nominal survival rates for female and male adults as well as the low temperature limit for nominal survival of larvae and pupae (Figure S6.2 c).

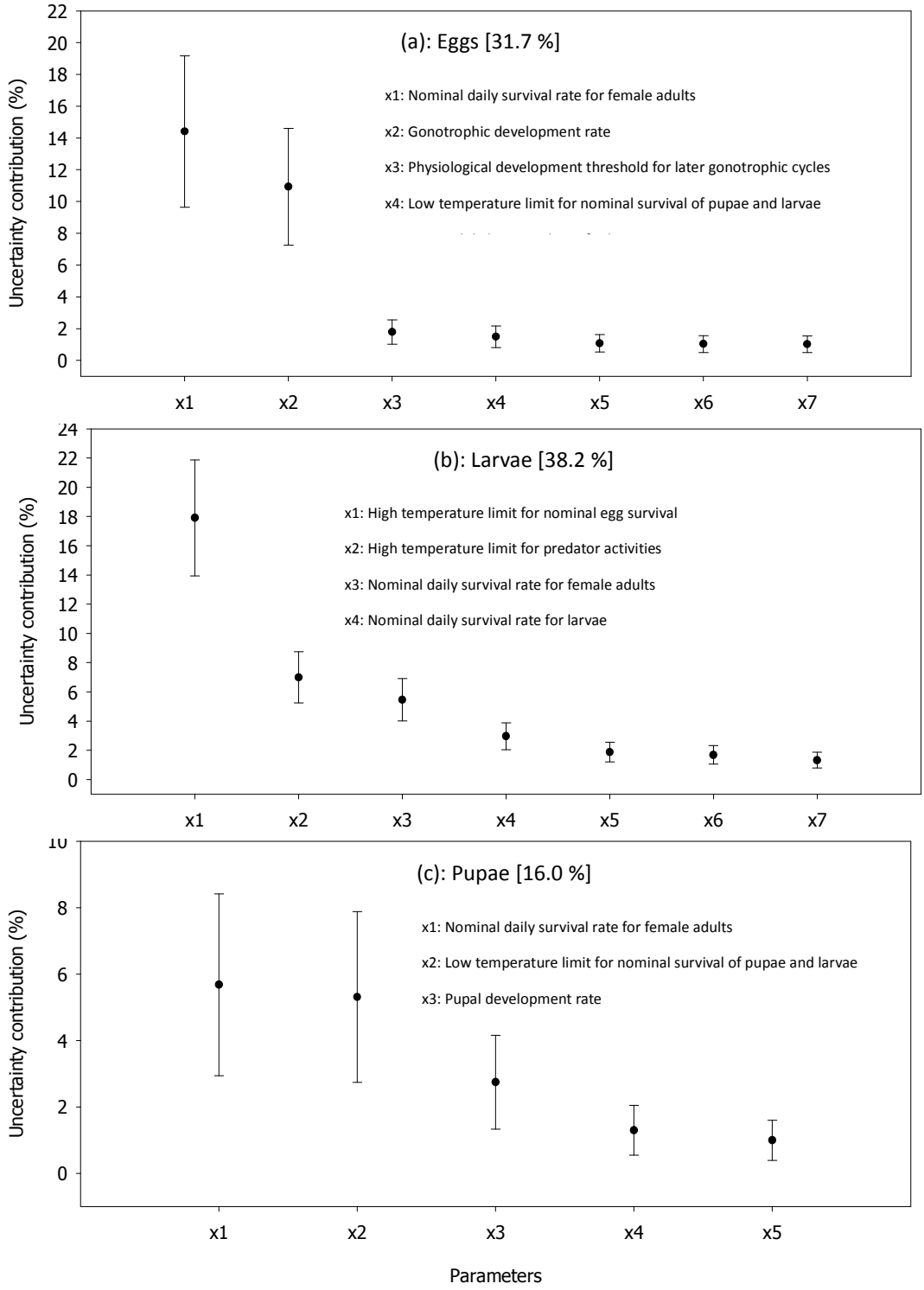

Figure S6.1 Uncertainty contributions by different model parameters for the temporal coefficient of variation (CV) of (a) eggs, (b) larvae and (c) pupae during the second simulation year. The vertical bars represent the 95% confidence intervals. The percentage values in brackets represent overall percentages of variance explained by the parameters shown in the figure.

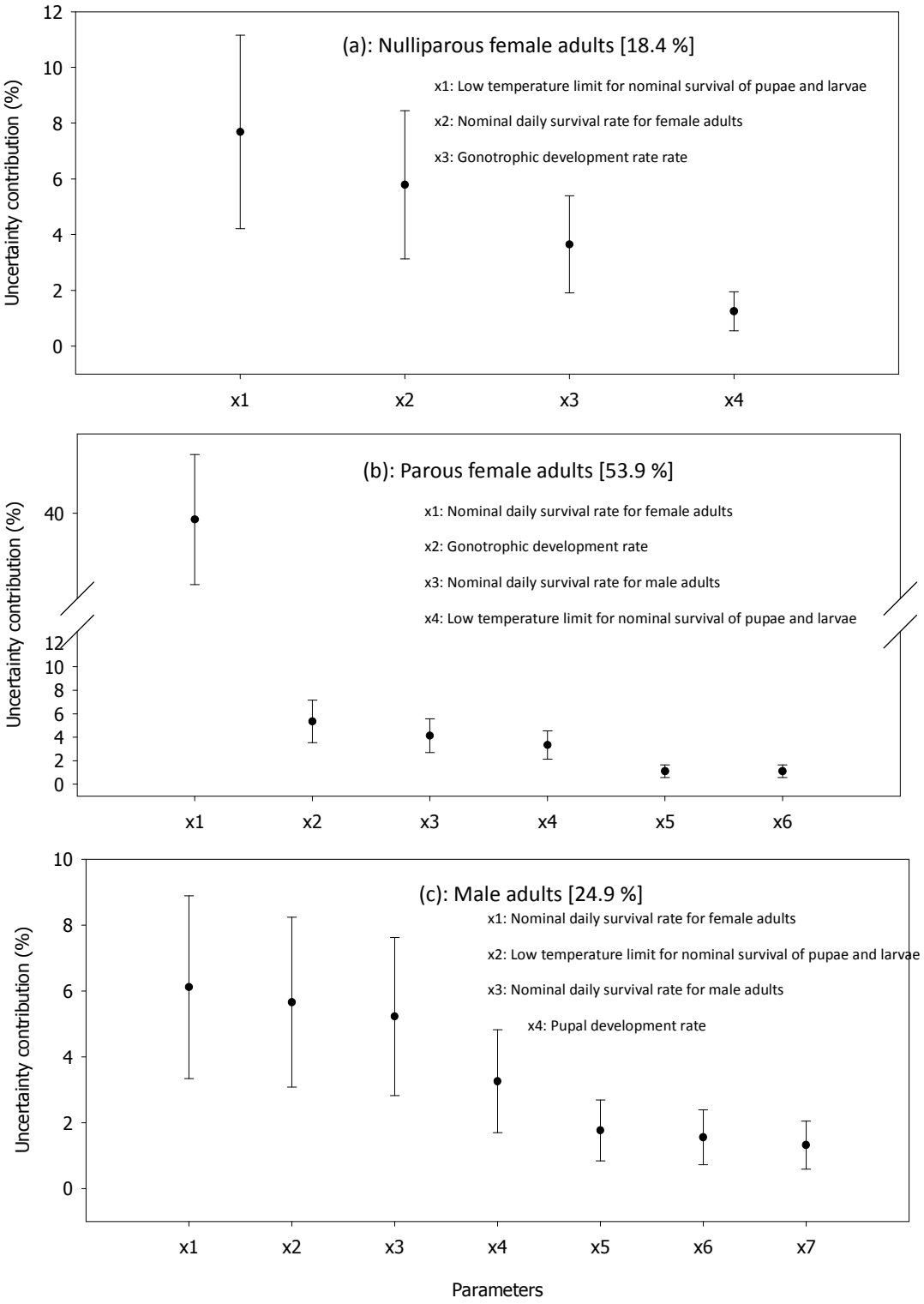

Figure S6.2 Uncertainty contributions by different model parameters for the temporal coefficients of variations of (a) nulliparous female adults, (b) parous female adults and (c) male adults during the second simulation year. The vertical bars represent the 95% confidence intervals. The percentage values in brackets represent overall percentages of variance explained by the parameters shown in the figure.

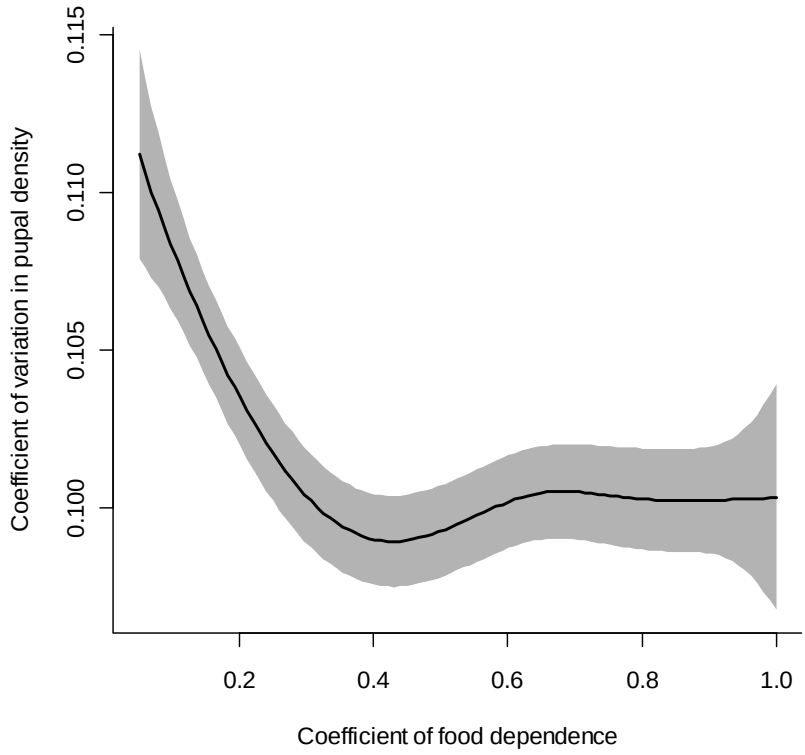

Figure S6.3 Dependence of temporal variability in population density at the community level on the coefficient of food dependence. The coefficient of food dependence accounts for about 1.3 % of uncertainty in temporal variability as measured by the temporal coefficient of variation during the second simulation year. The curves are fitted to the scatter plot of parameter values sampled by FAST and the corresponding predicted coefficient of variation in pupal density during the second simulation year using cubic smoothing splines with the SemiPar R package [1]. The shaded areas are the 95% confidence intervals of the fitted lines.

References

1. Wand MP, Coull BA, French JL, Ganguli B, Kammann EE, et al. (2005) SemiPar 1.0. R package. http://cran.r-project.org.

Text S7: Temporal variability of population density at the individual-house level

For uncertainty in the temporal CV (calculated with a time interval of 15 days instead of the daily interval due to the large data storage requirement for densities of each life stage over 730 days for 5000 simulations) of population density at the individual-house level, our results show that CVs are relatively high where there is low population density (Figure S7.1 a and S7.2 a). The nominal survival rates of female adults and larvae and the coefficient of metabolic weight loss, which are important parameters contributing to population density, are also important parameters contributing to temporal variability (Figure S7.1 b, c , d and Figure S7.2 b, c , d). In contrast to the temporal variability in population density at the community level, our results show that spatial dispersal can be an important parameter contributing to the temporal variability at the individual-house level (Figure S7.2 f), with higher spatial dispersal probability leading to lower temporal variability in the population dynamics (see Figure S7.3). Spatial dispersal also contributes to the temporal variability in pupal population density, but to a much lesser extent (see Figure S7.1 f). The coefficient of food dependence is very important for the temporal variability of pupal population density in houses with relatively small food input and relatively high egg density (see Figure S7.2 g), where there are stronger density-dependence effects on larval growth. The low temperature limit (10-20^{o}C) for nominal survival of pupae/larvae, which is important for temporal variability at the community level, is not detected as an important parameter at the individual-house level. This is due to the fact we use a longer time interval (15 days) to calculate the CVs, making occasional temporal variability (e.g., due to temperature falling below the low temperature limit for nominal survival of pupae and larvae) less detectable. Since the high temperature limit (25-35^{o}C) for predator-dependent egg survival is more frequently exceeded for

the weather in Iquitos, it is an important parameter contributing to temporal variability in population density at the individual-house level (Figure S7.2 e).

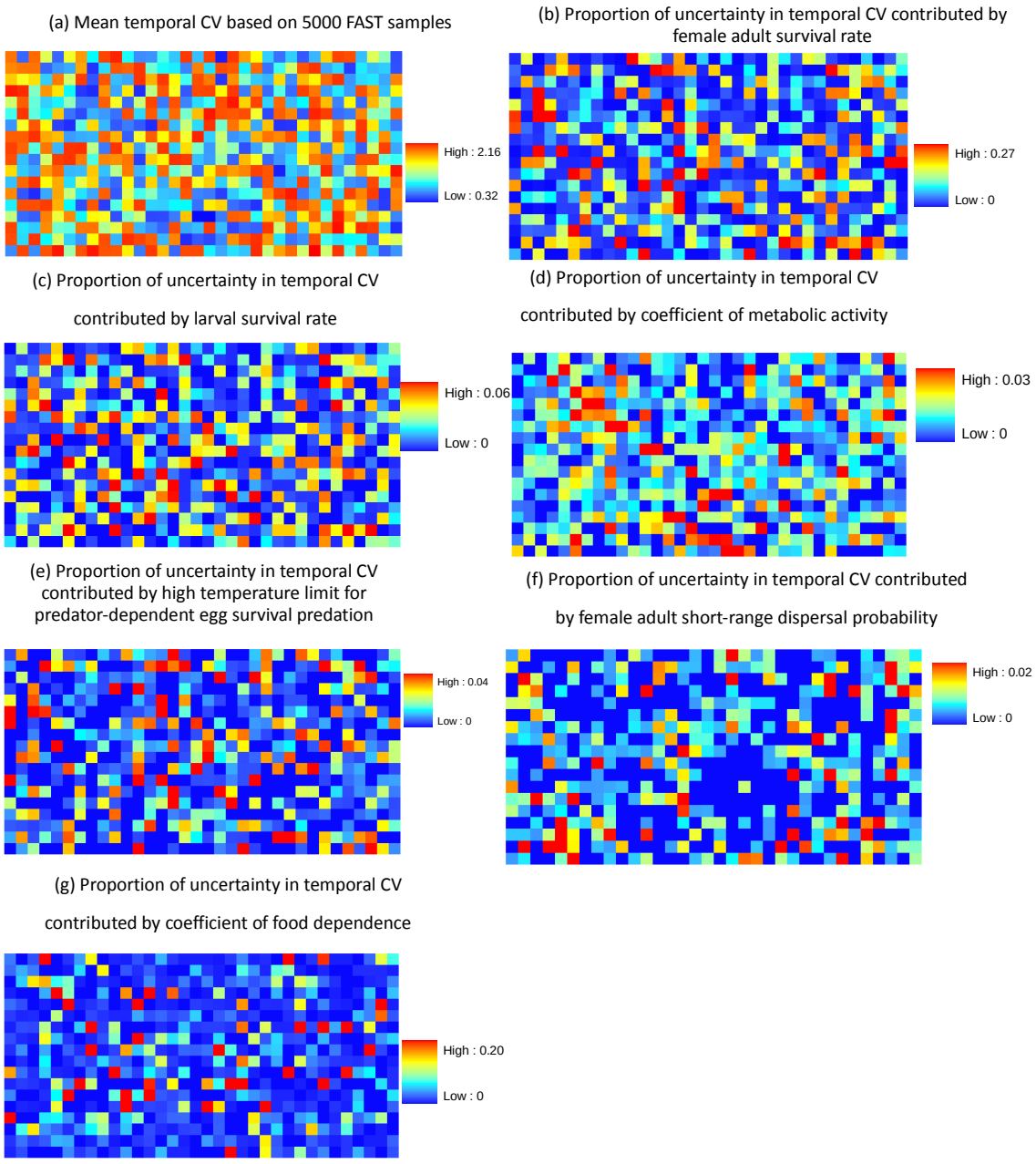

Figure S7.1 Mean temporal coefficient of variation (CV) for pupal population density at the individual-house level (a) and the proportion of uncertainty in CV contributed by different model parameters (b-g). To simplify this figure, only parameters with maximum uncertainty contributions larger than 0.03 are plotted except for panel (f) for the comparison of the importance of mosquito dispersal for different life stages. We did not plot the proportion of uncertainty in CV contributed by the nominal survival rate for male adults since the uncertainty contribution is mainly due to its correlation with the nominal survival rate for female adults.

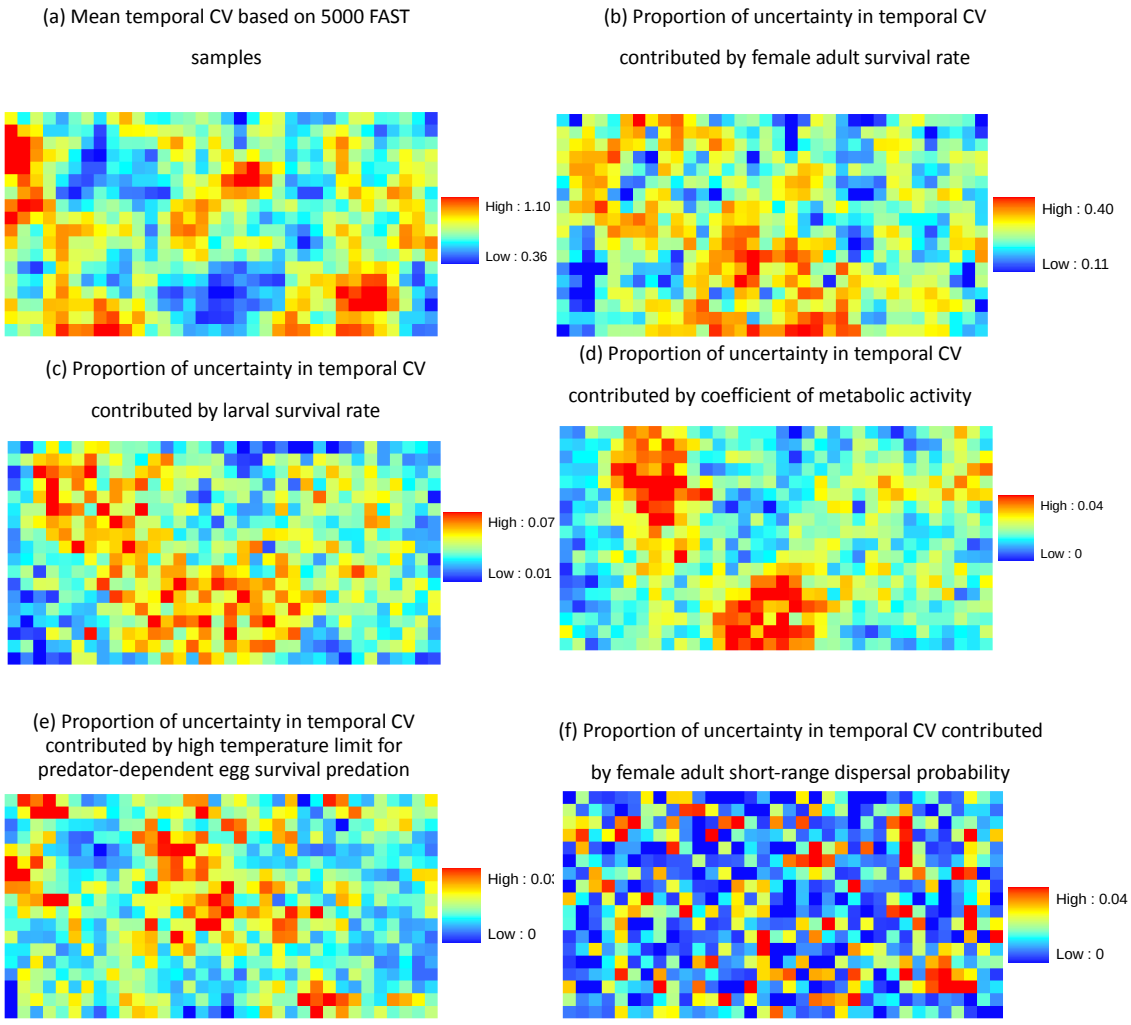

Figure S7.2 Mean temporal coefficient of variation (CV) for female adult population density at the individual-house level (a) and the proportion of uncertainty in CV contributed by different model parameters (b-f). To simplify this figure, only parameters with maximum uncertainty contributions larger than 0.03 are plotted. We did not plot the proportion of uncertainty in CV contributed by the nominal survival rate for male adults since the uncertainty contribution is mainly due to its correlation with the nominal survival rate for female adults.

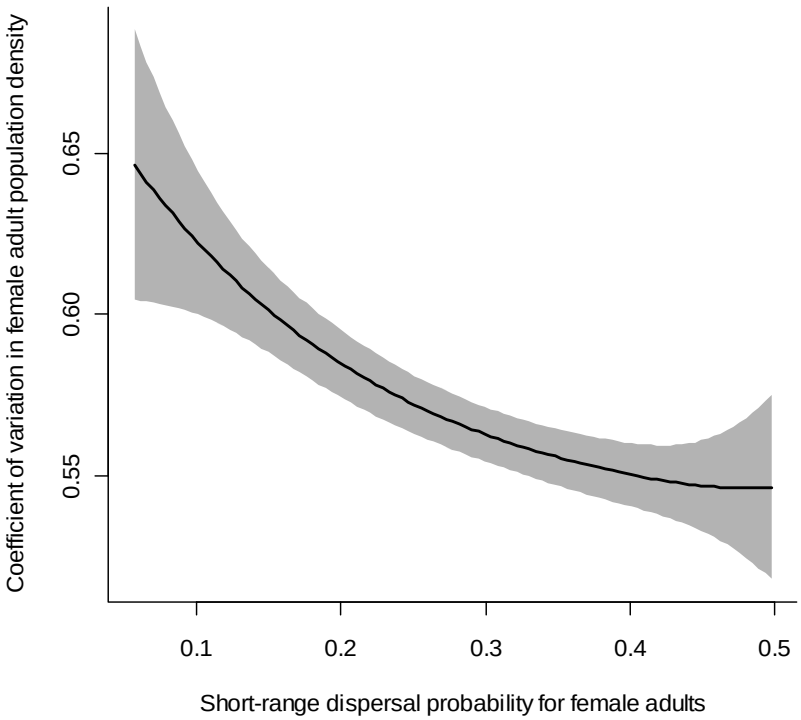

Figure S7.3 Dependence of temporal variability in female adult population density at an specific individual house (located at 4th row from top and 5th column from left) on short-range spatial dispersal. The short-range dispersal accounts for 3.8% of uncertainty in the temporal variability as measured by the temporal coefficient of variation during the second simulation year. The curves are fitted to the scatter plot of parameter values sampled by FAST and the corresponding predicted coefficient of variation in pupal density during the second simulation year using a cubic smoothing splines with the SemiPar R package [1]. The shaded areas are the 95% confidence intervals of the fitted lines.

References

1. Wand MP, Coull BA, French JL, Ganguli B, Kammann EE, et al. (2005) SemiPar 1.0. R package. http://cran.r-project.org.

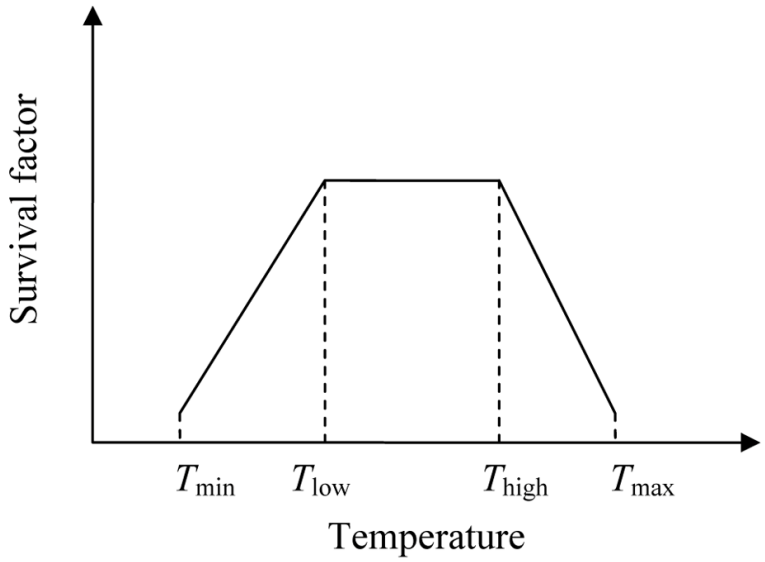

Figure S1.

Survival factor as a function of temperature. The survival factor ranges between 0 and 1 and is multiplied with nominal survival rate to get the temperature-dependent survival rate. T_{min} is the minimum temperature for survival, below which the low temperature has a strong effect on mosquito survival (the survival factor is generally less than 0.05); T_{low} is the low temperature limit below which is suboptimal for mosquito survival; T_{high} is the high temperature limit above which is suboptimal for mosquito surivival; T_{max} is the maximum temperature for survival, above which the high temperature has a very strong effect on mosquito survival (the survival factor is generally less than 0.05).

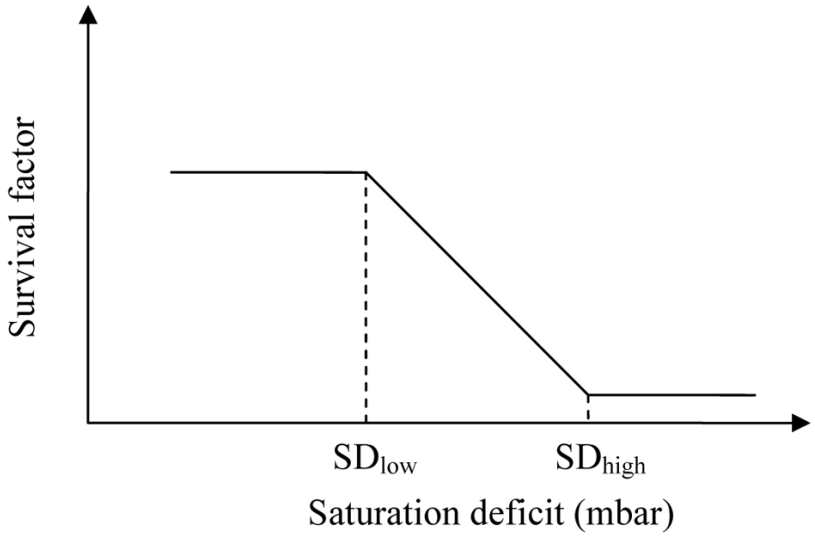

Figure S2.

Survival factor as a function of saturation deficit (SD). The survival factor ranges between 0 and 1 and is multiplied with nominal survival rate to get the humidity-dependent survival rate. SD_{low} is the low saturation deficit limit below which saturation deficit has little effect on mosquito survival. The survival rate decreases linearly between SD_{low} and SD_{high}, the high saturation deficit limit above which the saturation deficit has a strong effect on mosquito survival (survival factor is low).

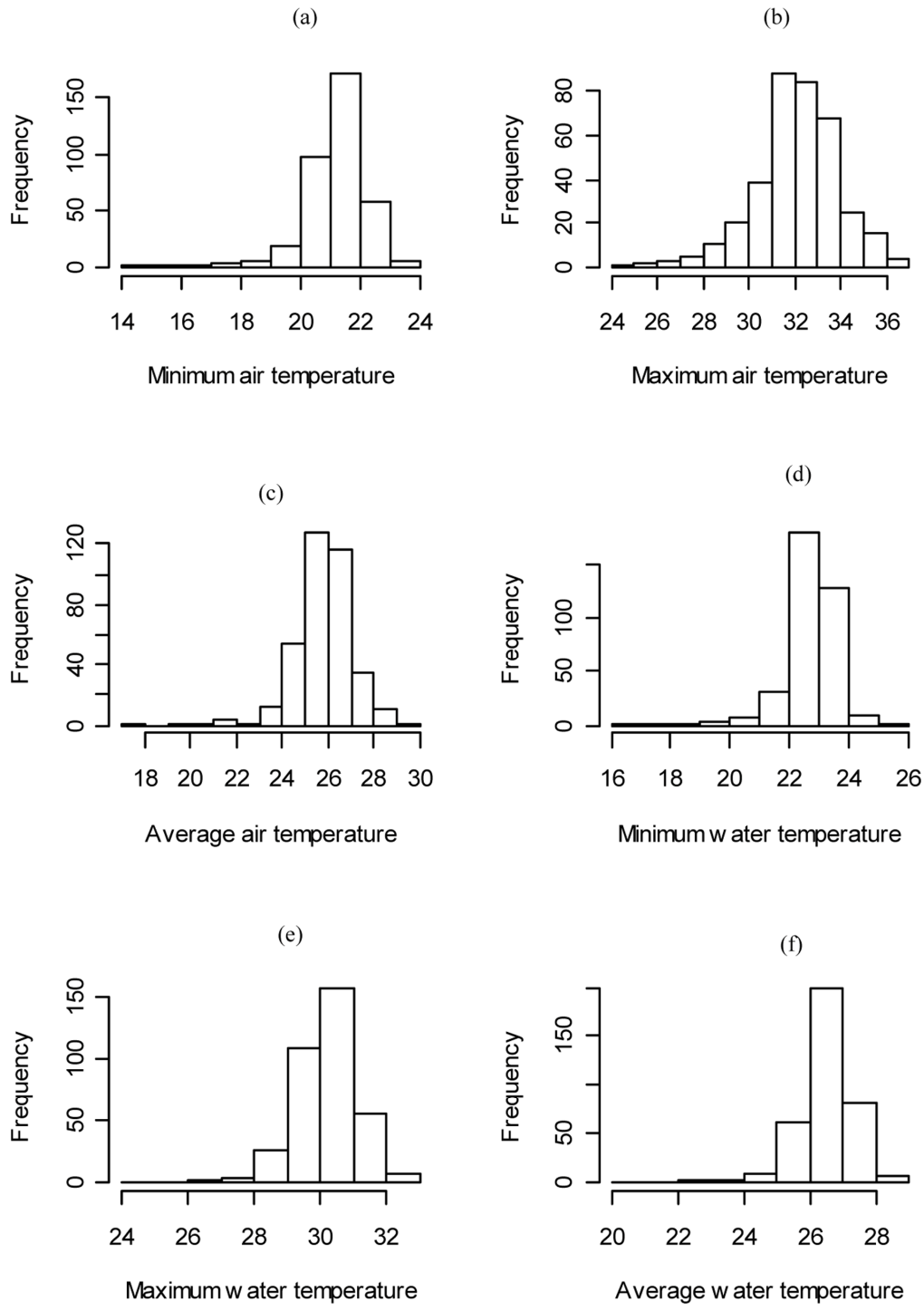

Figure S3.

Histograms of air and water temperatures (degrees Celsius) in Iquitos for year 2000. The container water temperatures are simulated using a polynomial function obtained from a regression of water temperature on air temperature and sun exposure for 12 containers monitored for 76 days in Gainesville, FL, USA [4]. The water temperature is calculated assuming a sun exposure of 0.5 for the container.

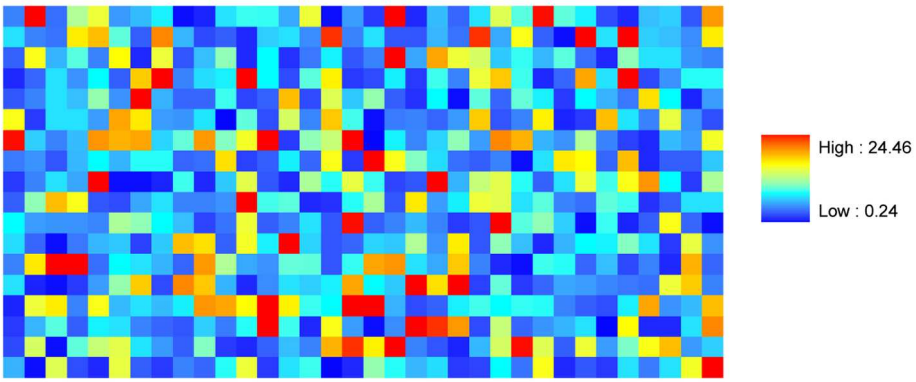

Figure S4.

Sum of daily food input from different containers (Unit: mg/day) at individual houses. Each block/cell represents a single house. The food inputs are fitted to the pupal data in the mosquito survey at individual houses in Iquitos [23]. The food inputs are not spatially clustered based on the Moran's I statistic [46] using inverse distance weights (I = 0.005, p-value = 0.82).

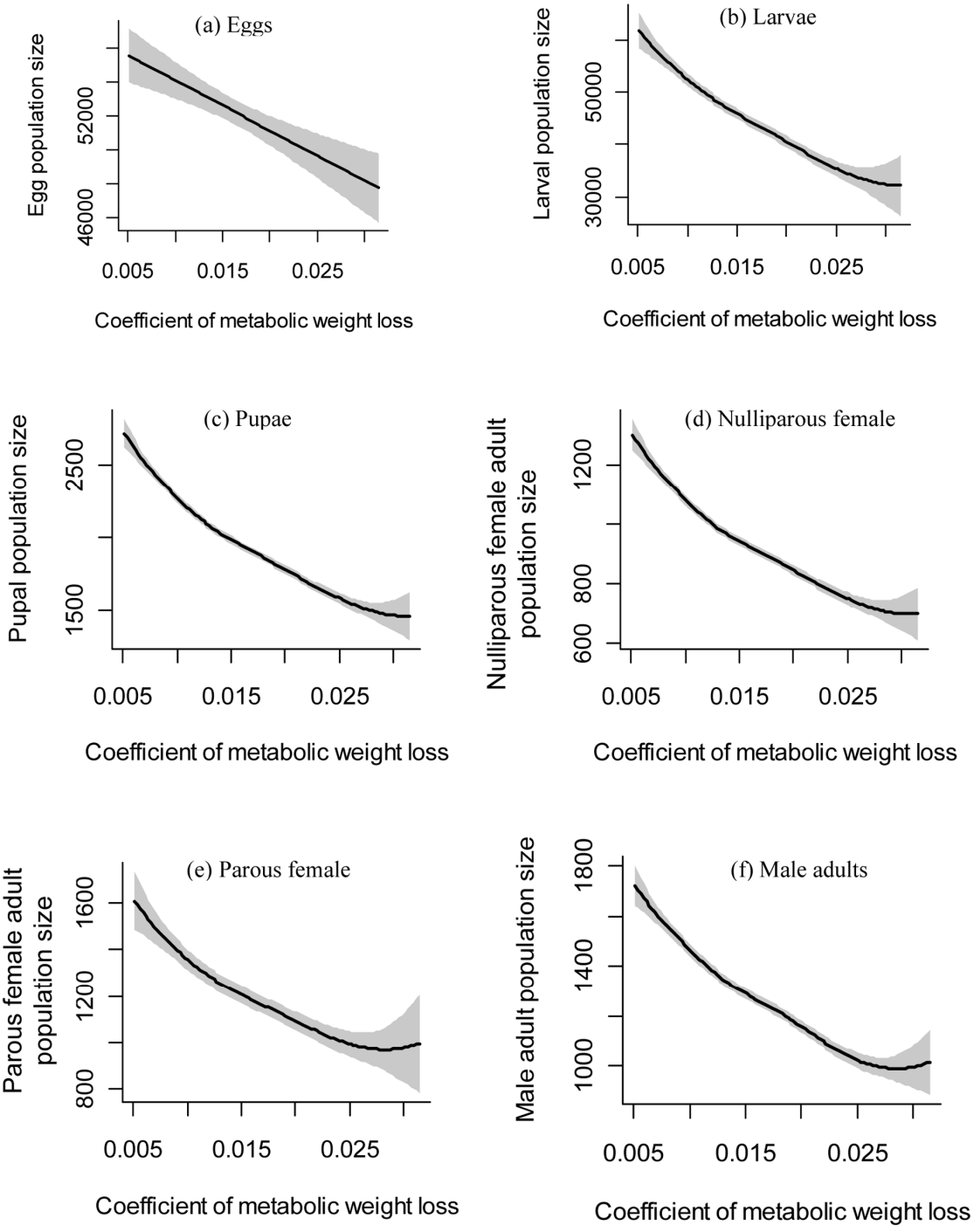

Figure S5.

Dependence of community-level population density on coefficient of metabolic weight loss at different life stages. The curves are fitted to the scatter plot of parameter values sampled by FAST and the corresponding predicted population densities using cubic smoothing splines with the SemiPar R package [45]. The shaded areas are the 95% confidence intervals of the fitted lines.

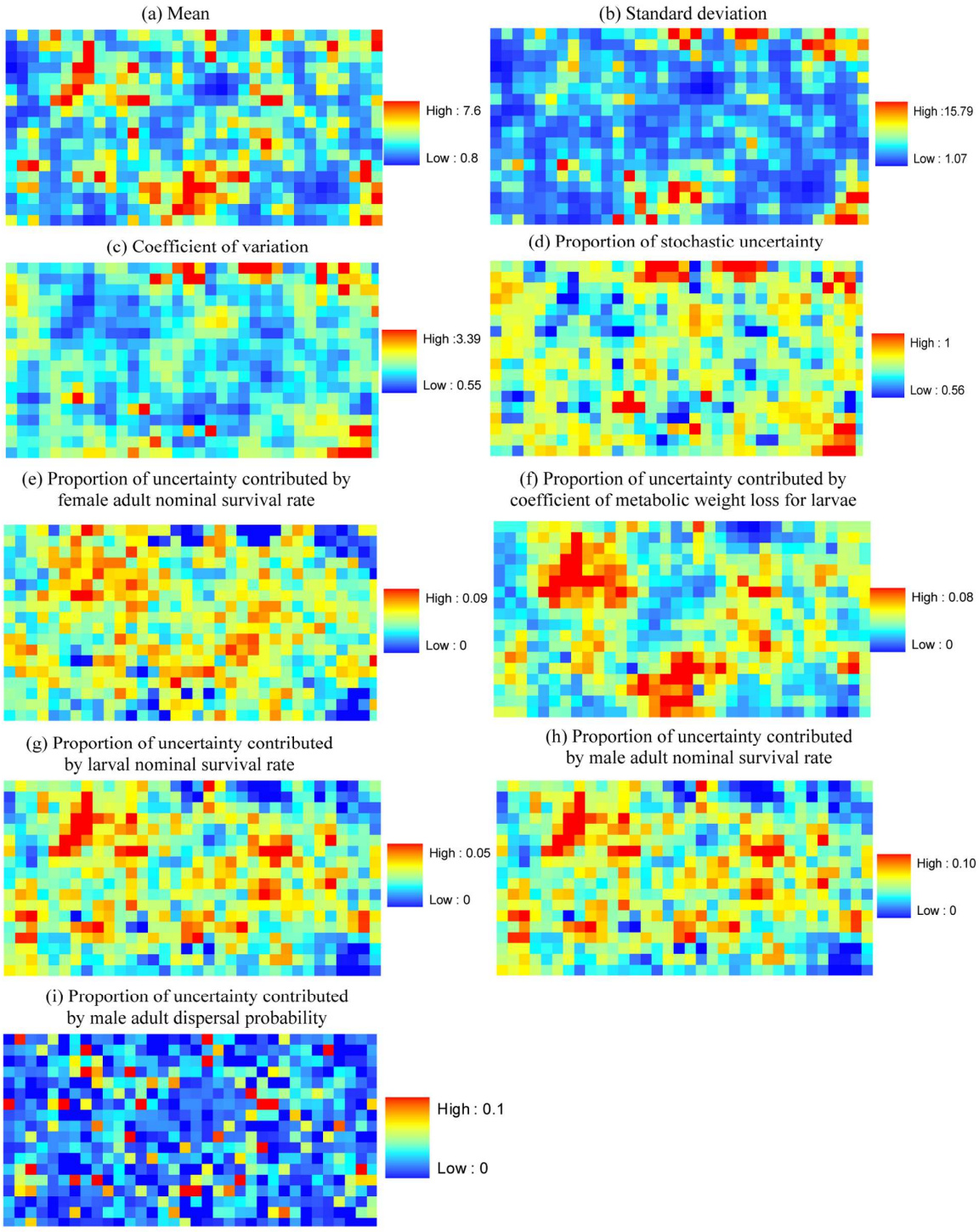

Figure S6. Uncertainty in the predicted male adult population density at the individual-house level on simulation day 720. For each individual house, we quantify uncertainty in the predicted population density (as is jointly described by the (a) mean, (b) standard deviation, and (c) coefficient of variation of predicted population density across the parameter sets sampled by FAST), (d) the proportion of uncertainty contributed by stochasticity, and (e–i) the proportions of uncertainty contributed by specific model parameters. To simplify this figure, only parameters with uncertainty contributions in any house larger than 5% are plotted.

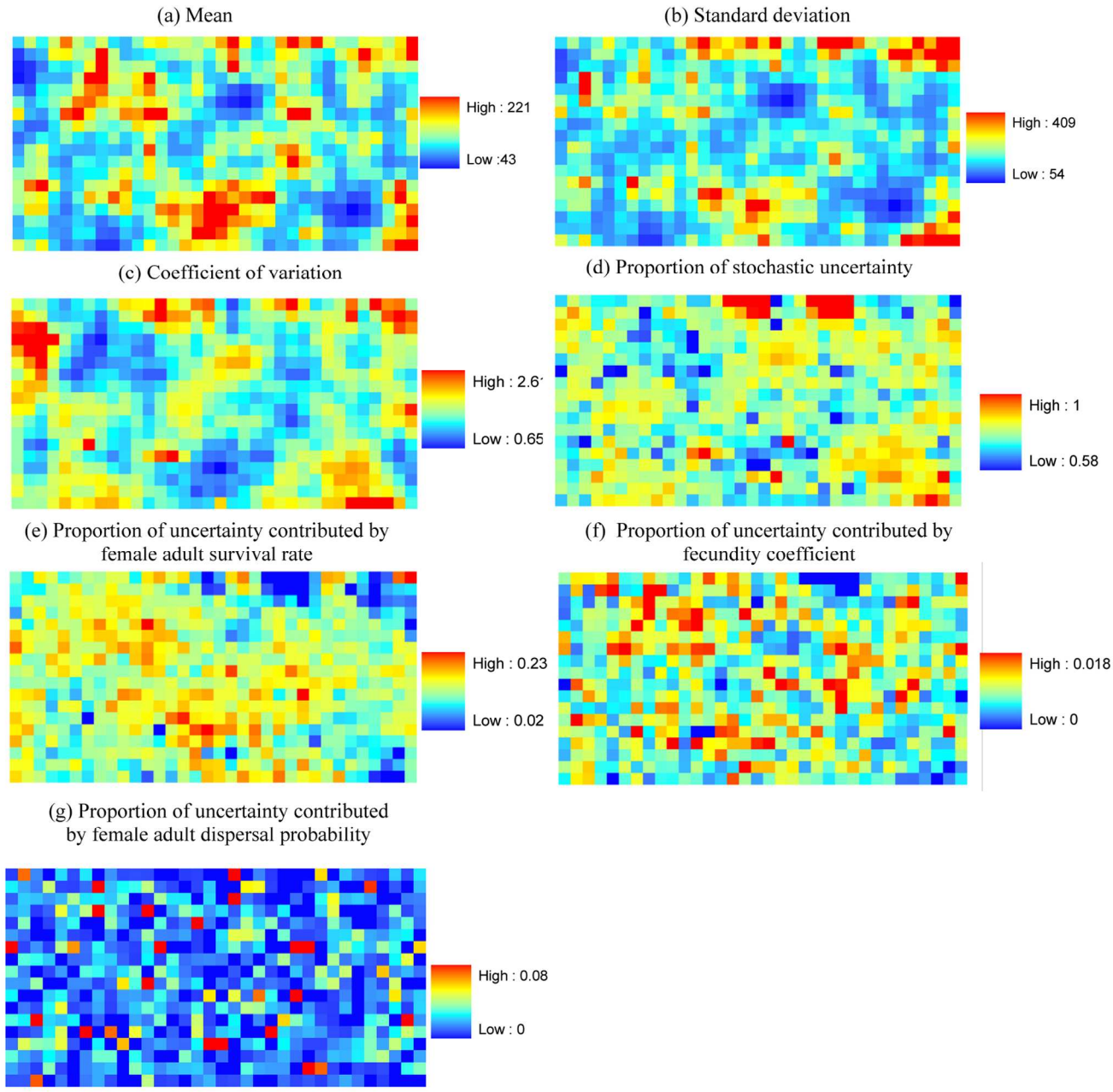

Figure S7.

Uncertainty in the predicted egg density at the individual-house level on simulation day 720. For each individual house, we quantify uncertainty in the predicted population density (as is jointly described by the (a) mean, (b) standard deviation, and (c) coefficient of variation of predicted population density across the parameter sets sampled by FAST), (d) the proportion of uncertainty contributed by stochasticity, and (e–g) the proportions of uncertainty contributed by specific model parameters. To simplify this figure, only parameters with uncertainty contributions in any house larger than 5% are plotted.

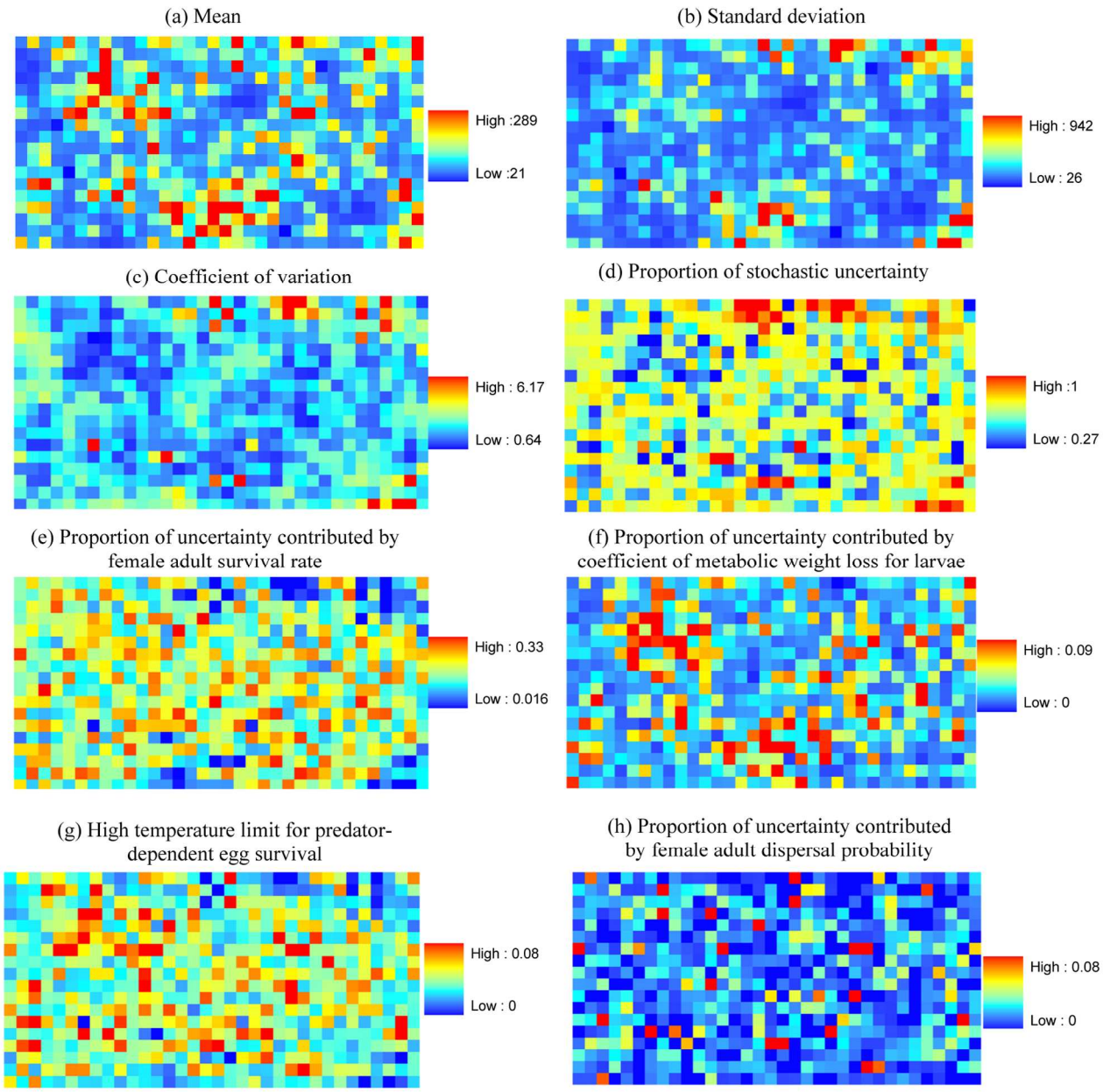

Figure S8.

Uncertainty in the predicted larval population density at the individual-house level on simulation day 720. For each individual house, we quantify uncertainty in the population density (as is jointly described by the (a) mean, (b) standard deviation, and (c) coefficient of variation of predicted population density across the parameter sets sampled by FAST), (d) the proportion of uncertainty contributed by stochasticity, and (e–g) the proportions of uncertainty contributed by specific model parameters. To simplify this figure, only parameters with uncertainty contributions in any house larger than 5% are plotted.

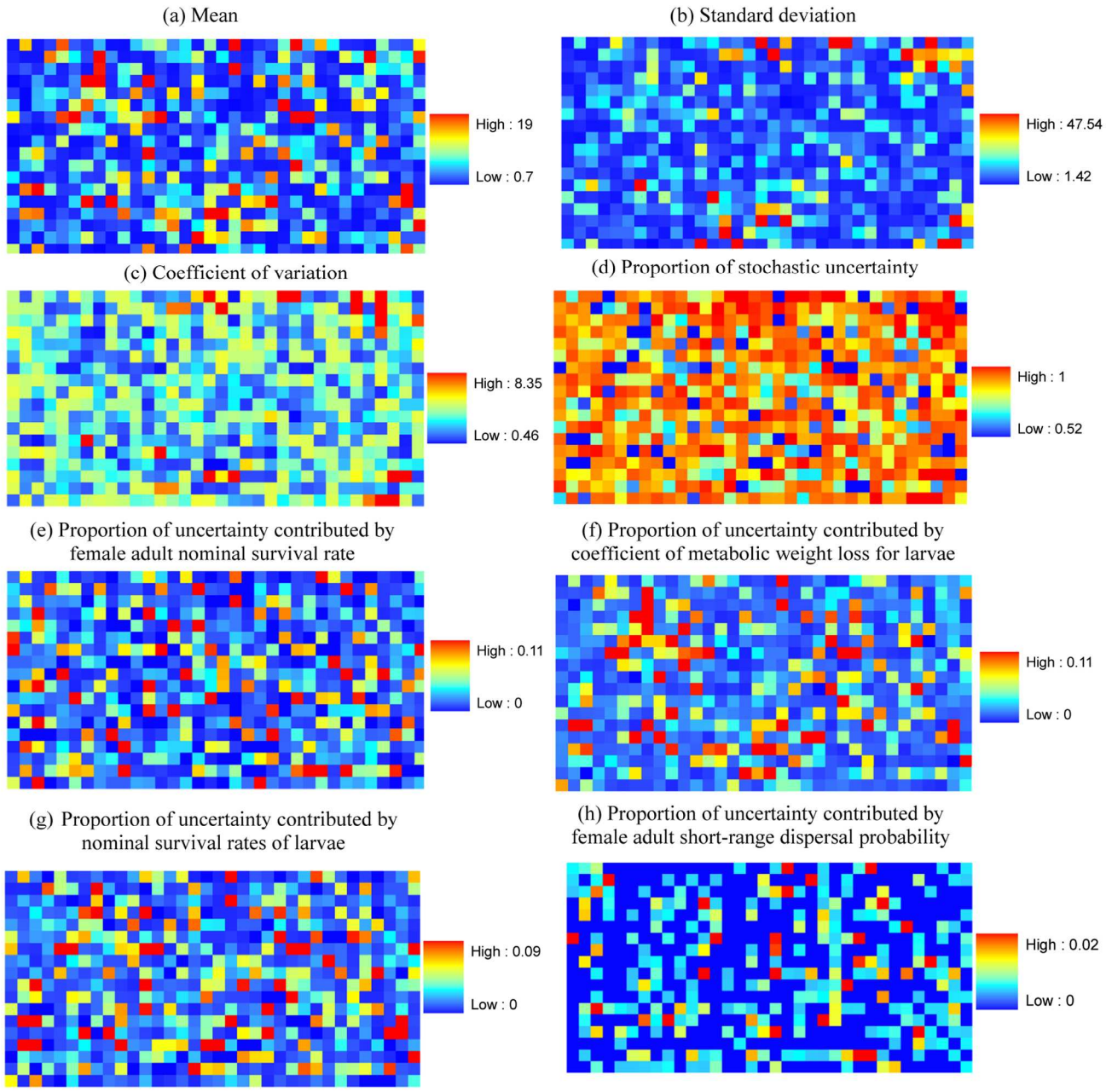

Figure S9.

Uncertainty in the predicted pupal density at the individual-house level on simulation day 720. For each individual house, we quantify uncertainty in the predicted population density (as is jointly described by the (a) mean, (b) standard deviation, and (c) coefficient of variation of predicted population density across the parameter sets sampled by FAST), (d) the proportion of uncertainty contributed by stochasticity, and (e–h) the proportions of uncertainty contributed by specific model parameters. To simplify this figure, only parameters with maximum uncertainty contributions larger than 5% in any house are plotted except for panel (h), which is shown for the comparison of mosquito dispersal importance at different life stages.

Table S1 Uncertainties in the estimates of parameters for adults (15 parameters).

Parameter	Description	Lower Range	Upper Range	Default Value	Confidence for default value	Sources
A-FS	Nominal survival rate for female adults	0.75	0.99	0.89	Moderate	[1,2,3,4,5],, Workshop
A-MS	Nominal survival rate for male adults	0.72	0.99	0.77	Moderate	[1,2,3,4,5], Workshop
A-TL	Low temperature limit for nominal survival (^{o}C)	2	10	4	Low	[6], Workshop
A-TH	High temperature limit for nominal survival (^{o}C)	35	40	39	Low	[6], Workshop
A-TMN	Minimum temperature for survival (^{o}C)	-5	2	0	Low	[6,7], Workshop
A-TMX	Maximum temperature for survival (^{o}C)	40	45	44	Low	[6]
A-SDL	Low saturation deficit limit for survival (mBar)	5	20	10	Low	[6,7], Workshop
A-SDH	High saturation deficit limit for survival (mBar)	25	35	30	Low	[6], Workshop
A-STMN	Survival factor at the minimum temperature limit for survival	0	0.05	0.05	No	Workshop
A-STMX	Survival factor at the maximum temperature limit for survival	0	0.05	0.05	No	Workshop
A-SSDH	Survival factor for saturation deficits higher than *SDH*	0.55	0.95	0.6	Low	[6], Workshop
A-OVTMN	Minimum temperature for oviposition (^{o}C)	17	24	18	Low	[8], Workshop
A-F	Coefficient of fecundity (number of eggs per mg wet-weight of female adults)	35	55	46.5	Low	[8]
A-DPTG	Development percentage threshold for subsequent gonotrophic cycles	0.5	0.7	0.58	Low	[5,9,10], Workshop
A-FWC	Conversion coefficient from dry weight to wet weight for female adults	1.45	1.8	1.655	Low	[8], Workshop

*Fecundity per gonotrophic cycle is assumed to be linearly related to the wet weight of a female adult. Namely, Fecundity = A-F$\times W_{female,}$ where W_{female} is the wet weight of a female adult.

References:

1. Maciel-De-Freitas R, Codego CT, Lourenco-De-Oliveira R (2007) Body size-associated survival and dispersal rates of *Aedes aegypti* in Rio de Janeiro. Med Vet Entomol 21: 284-292.
2. McDonald PT (1977) Population characteristics of domestic *Aedes aegypti* (Diptera: Culicidae) in villages on Kenya coast. 1. Adult survival and population size. J Med Entomol 14: 42-48.
3. Sheppard PM, Macdonal.Ww, Tonn RJ, Grab B (1969) Dynamics of an adult population of *Aedes aegypti* in relation to dengue haemorrhagic fever in Bangkok. J Anim Ecol 38:

661-702.

4. Harrington LC, Vermeylen F, Jones JJ, Kitthawee S, Sithiprasasna R, et al. (2008) Age-dependent survival of the dengue vector *Aedes aegypti* (Diptera : Culicidae) demonstrated by simultaneous release-recapture of different age cohorts. J Med Entomol 45: 307-313.
5. Harrington LC, Edman JD, Scott TW (2001) Why do female *Aedes aegypti* (Diptera: Culicidae) feed preferentially and frequently on human blood? J Med Entomol 38: 411-422.
6. Christophers SR (1960) *Aedes aegypti* (L.), the yellow fever mosquito. Cambridge, UK: Cambridge University Press.
7. MacFie JWS (1920) Heat and *Stegomyia fasciata*, short exposures to raised temperatures. Ann Trop Med Parasitol 14: 73-82.
8. Focks DA, Haile DG, Daniels E, Mount GA (1993) Dynamic life table model of *Aedes aegypti* (Diptera: Culicidae) - Analysis of the literature and model development. J Med Entomol 30: 1003-1017.
9. Jalil M (1974) Observations on the fecundity of Aedes triseriatus (Diptera: Culicidae). Entomol Exp Appl 17: 223-233.
10. Nayar JK, Sauerman DM (1975) The effects of nutrition on survival and fecundity in Florida mosquitoes. Part. 3. Utilization of blood and sugar for fecundity. J Med Entomol 12: 220-225.

Table S2 Uncertainties in the estimates of parameters for larvae and pupae (14 parameters).

Parameter	Description	Lower Range	Upper Range	Default Value	Confidence for default value	Sources
L-S	Nominal survival rate for larvae	0.9	1.0	0.99	Low	[1], Workshop
P-S	Nominal survival rate for pupae	0.9	1.0	0.99	Low	[2], Workshop
LP-TL	Low temperature limit for nominal survival of larvae and pupae (^{o}C)	10	20	15	Moderate	[2], Workshop
LP-TH	High temperature limit for nominal survival of larvae and pupae (^{o}C)	30	40	39	Low	[2,3], Workshop
LP-TMN	Minimum temperature for survival of larvae and pupae (^{o}C)	5	10	8	Moderate	[4], Workshop
LP-TMX	Maximum temperature for survival of larvae and pupae (^{o}C)	40	46	44	Low	Workshop
LP-STMN	Survival factor at the minimum temperature limit	0	0.05	0.05	No	Workshop
LP-STMX	Survival factor at the maximum temperature limit	0	0.05	0.05	No	Workshop
P-SEM	Emergence probability for pupae	0.75	0.9	0.83	Low	[3,4,5], Workshop
LP-SLIP	Survival of larvae with lipid reserve under fasting	0.9	1	0.95	Low	[6], Workshop
LP-SNLIP	Survival of larvae without lipid reserve under fasting	0.3	0.7	0.5	Low	[1], Workshop
L-Sp	Larval survival probability at pupation	0.9	1	0.95	Low	[1], Workshop
L-Wp	Minimum weight for pupation (mg)	0.1	0.19	0.1	Moderate	[1]
L-SDRY	Larval survival probability at dry container	0	0.05	0.05	No	Workshop

References

1. Focks DA, Haile DG, Daniels E, Mount GA (1993) Dynamic life table model of *Aedes aegypti* (Diptera: Culicidae) - Analysis of the literature and model development. J Med Entomol 30: 1003-1017.
2. Chang LH, Hsu EL, Teng HJ, Ho CM (2007) Differential survival of *Aedes aegypti* and *Aedes albopictus* (Diptera : Culicidae) larvae exposed to low temperatures in Taiwan. J Med Entomol 44: 205-210.
3. Tsuda Y, Takagi M (2001) Survival and development of *Aedes aegypti* and *Aedes albopictus* (Diptera: Culicidae) larvae under a seasonally changing environment in Nagasaki, Japan. Environ Entomol 30: 855-860.
4. Rueda LM, Patel KJ, Axtell RC, Stinner RE (1990) Temperature-dependent development and survival rates of *Culex quinquefasciatus* and *Aedes aegypti* (Diptera: Culicidae). J Med Entomol 27: 892-898.
5. Tun-Lin W, Burkot TR, Kay BH (2000) Effects of temperature and larval diet on development rates and survival of the dengue vector *Aedes aegypti* in north Queensland, Australia.

Med Vet Entomol 14: 31-37.
6. Southwood TRE, Tonn RJ, Yasuno M, Reader PM, Murdie G (1972) Studies on life budget of *Aedes aegypti* in Wat Samphaya, Bangkok, Thailand. Bull WHO 46: 211-226.

Table S3 Uncertainties in the estimates of parameters for egg survival and hatching (19 parameters).

Parameter	Description	Lower Range	Upper Range	Default Value	Confidence for default value	Sources
E-S	Nominal survival rate for eggs	0.95	1.0	0.99	Low	Workshop
E-TL	Low temperature limit for nominal survival (°C)	-6	5	-6	Low	[1,2], Workshop
E-TH	High temperature limit for nominal survival (°C)	28	35	30	Low	[3], Workshop
E-TMN	Minimum temperature for survival (°C)	-14	-6	-14	Low	[3,4], Workshop
E-TMX	Maximum temperature for survival (°C)	40	45	44	Low	[3]
E-SDL	Low saturation deficit limit for survival (mBar)	5	20	10	Low	[3,4]
E-SDH	High saturation deficit limit for survival (mBar)	25	35	30	Low	[3]
$E\text{-}SE_{high}$	High sun exposure limit for survival in dry containers (proportion)	0.6	0.9	0.85	Low	[3], Workshop
E-STMN	Survival factor at temperatures lower than minimum temperature limit for survival	0	0.05	0.05	No	Workshop
E-STMX	Survival factor at temperature higher than maximum temperature limit for survival	0	0.05	0.05	No	Workshop
E-SSDH	Survival factor for saturation deficits higher than *SDH* for containers with low sun exposure	0.75	0.99	0.95	Low	[5], Workshop
E-SSEH	Survival factor for sun exposure higher than E-*SEH* for dry container	0.75	0.99	0.95	Low	[5], Workshop
E-PTL	Low temperature limit for predator activities (°C)	15	25	20	Low	[5], Workshop
E-PTH	High temperature limit for predator activities (°C)	25	35	30	Low	[3], Workshop
E-SPTL	Survival factor for predation at low temperatures (< *E-PTL*)	0.95	1	0.99	No	[3,4], Workshop
E-SPTH	Survival factor for predation at high temperatures (> *E-PTH*)	0.65	0.9	0.7	Low	[5], Workshop
E-HTMN	Minimum temperature for hatching (°C)	14	22	22	Low	[5] Workshop
E-HPNF	Hatching probability without	0	0.25	0.2	Moderate	[3,6], Workshop

E-HPF	flooding Hatching probability with flooding	0.3	0.65	0.6	Moderate	[5], Workshop

References:

1. Focks DA, Haile DG, Daniels E, Mount GA (1993) Dynamic life table model for *Aedes aegypti* (Diptera: Culicidae) - Simulation and validation. J Med Entomol 30: 1018-1028.
2. Gilpin ME, McClelland GAH (1979) Systems-analysis of the yellow fever mosquito *Aedes aegypti*. Forts Zool 25: 355-388.
3. Christophers SR (1960) *Aedes aegypti* (L.), the yellow fever mosquito. Cambridge, UK: Cambridge University Press.
4. MacFie JWS (1920) Heat and *Stegomyia fasciata*, short exposures to raised temperatures. Ann Trop Med Parasitol 14: 73-82.
5. Focks DA, Haile DG, Daniels E, Mount GA (1993) Dynamic life table model of *Aedes aegypti* (Diptera: Culicidae) - Analysis of the literature and model development. J Med Entomol 30: 1003-1017.
6. Hien DS (1975) Biology of *Aedes aegypti* (L., 1762) and *Aedes albopictus* (Skuse, 1895) (Diptera, Culicidae) II. Effect Of environmental conditions on the hatching of larvae. Acta Parasitol Pol 23: 537-552

Table S4 Uncertainties in the estimates of parameters for larval weight gain (8 parameters).

Parameter	Description	Lower Range	Upper Range	Default Value	Confidence for default value	Sources
Fa	Conversion rate of consumed food to biomass	0.28	0.38	0.30	Moderate	Figure 11 in [1], Workshop
Fb	Exponent of body weight	0.75	0.85	0.8	Moderate	Figure 11 in [1] Workshop
Fc	Coefficient of food dependence	0.05	1.0	0.1	No	Figure 11 in [1]
Fd1	Coefficient of metabolic weight loss	0.005	0.032	0.016	Low	Workshop
Fd2	Exponent of metabolic activity	0.59	0.73	0.667	Moderate	[1], Workshop
FL_a	Intercept for lipid prediction	0.041	0.071	0.056	0.0073*	Figure 13 in [1]
FL_b	Slope for lipid prediction	0.255	0.303	0.279	0.012 *	Figure 13 in [1]
FF_l	Proportion of dead larvae to liver powder	0.25	0.5	0.4	Low	Figure 15 in [1]

*Note: For parameters assumed to follow a normal distribution, the “lower range” and “upper range” refer to the 95% confidence interval and the value in the confidence column refers to the estimated standard error.

References

1. Gilpin ME, McClelland GAH (1979) Systems-analysis of the yellow fever mosquito *Aedes aegypti*. Forts Zool 25: 355-388.

Table S5 Uncertainties in the estimates of parameters for mosquito dispersal (7 parameters)

Parameter	Description	Lower Range	Upper Range	Default Value	Confidence for default value	Sources
SD-FS	Short-range dispersal probability for female adults	0.05	0.5	0.3	Low	[1], Workshop
SD-MS	Short-range dispersal probability for male adults	0.05	0.5	0.3	Low	[2,3], Workshop
SD-FL	Long-range dispersal probability for female adults	0	0.1	0.02	Low	[2,3], Workshop
SD-ML	Long-range dispersal probability for male adults	0	0.1	0.02	Low	[3], Workshop
SD-FES	Short-range dispersal probability for female adults in empty house	0.1	0.9	0.8	Low	[3], Workshop
SD-PES	Short-range dispersal probability for male adults in empty house	0.1	0.9	0.8	Low	[3], Workshop
SD-LD	Distance for long range dispersal (house-distance)	5	20	10	Low	[3], Workshop

References:

1. Gilpin ME, McClelland GAH (1979) Systems-analysis of the yellow fever mosquito *Aedes aegypti*. Forts Zool 25: 355-388.
2. Harrington LC, Scott TW, Lerdthusnee K, Coleman RC, Costero A, et al. (2005) Dispersal of the dengue vector *Aedes aegypti* within and between rural communities. Am J Trop Med Hyg 72: 209-220.
3. Magori K, Legros M, Puente ME, Focks DA, Scott TW, et al. (2009) Skeeter Buster: a stochastic, spatially-explicit modeling tool for studying *Aedes aegypti* population replacement and population suppression strategies. Plos Neglect Trop Dis 3: e508.

Table S6 Uncertainty contributions (%) by different model parameters for predicted egg population density at the community level

Parameters	Descriptions	Uncertainty contribution	Standard error
A-FS	Nominal daily survival rate for female adults	71.75	2.42
A-MS	Nominal daily survival rate for male adults	6.56	0.55
A-F	Coefficient of fecundity for female adults	2.60	0.34
L-S	Nominal daily survival rate for larvae	2.56	0.34
Fc	Coefficient of food dependence for larvae	1.75	0.28
A-D	Gonotrophic development rate	1.65	0.27
P-S	Nominal daily survival rate for pupae	1.31	0.24
A-FWC	Conversion coefficient from dry weight to wet weight for female adults	1.06	0.21

Note: Only parameters that contribute more than one percent to the uncertainty are shown in the table. They explain 89.2% of uncertainty in the predicted population density.

Table S7 Uncertainty contributions (%) by different model parameters for predicted larval population density at the community level

Parameters	Descriptions	Uncertainty contribution	Standard error
A-FS	Nominal daily survival rate for female adults	39.42	1.54
E-PTH	High temperature limit for predator activities on eggs	9.48	0.67
Fd1	Coefficient of metabolic weight loss for larvae	7.66	0.59
L-S	Nominal daily survival rate for larvae	5.60	0.50
A-MS	Nominal daily survival rate for male adults	4.27	0.43
E-SPTH	Survival factor of predation at high temperatures for egg	3.73	0.40
E-TH	High temperature limit for nominal egg survival	3.09	0.37
E-PTL	Low temperature limit for predator activities on eggs	2.79	0.35
E-D	Embryonic development rate	1.79	0.28
P-S	Nominal daily survival rate for pupae	1.38	0.24
A-D	Gonotrophic development rate	1.05	0.21

Note: Only parameters that contribute more than one percent to the uncertainty are shown in the table. They explain 80.3% of uncertainty in the predicted population density.

Table S8 Uncertainty contributions (%) by different model parameters for predicted pupal population density at the community level

Parameters	Descriptions	Uncertainty contribution	Standard error
Fd1	Coefficient of metabolic weight loss for larvae	20.50	1.05
L-S	Nominal daily survival rate for larvae	17.37	0.95
A-FS	Nominal daily survival rate for female adults	14.18	0.85
L-D	Larval development rate	7.14	0.58
E-PTH	High temperature limit for predator activities on eggs	3.72	0.41
P-D	Pupal development rate	3.23	0.38
P-S	Nominal daily survival rate for pupae	3.23	0.38
Fa	Conversion rate of consumed food to biomass for larvae	2.91	0.36
A-MS	Nominal daily survival rate for male adults	1.61	0.25
Fc	Coefficient of food dependence for larvae	1.34	0.24
E-SPTH	Survival factor for predation at high temperatures	1.21	0.23

Note: Only parameters that contribute more than one percent to the uncertainty are shown in the table. They explains 77.6% of uncertainty in the predicted population density.

Table S9 Uncertainty contributions (%) by different model parameters for the predicted population density of nulliparous female adults at the community level

Parameters	Descriptions	Uncertainty contribution	Standard error
A-FS	Nominal daily survival rate for female adults	24.50	1.17
L-S	Nominal daily survival rate for larvae	17.84	0.97
Fd1	Coefficient of metabolic weight loss for larvae	16.42	0.92
L-D	Larval development rate	6.06	0.53
P-S	Nominal daily survival rate for pupae	5.51	0.50
E-PTH	High temperature limit for predator activities on eggs	2.52	0.33
A-MS	Nominal daily survival rate for male adults	2.39	0.31
Fa	Conversion rate of consumed food to biomass for larvae	2.28	0.32
P-SEM	Emergence probability for pupae	2.28	0.32
A-D	Gonotrophic development rate	1.10	0.22
L-Sp	Larval survival probability at pupation	1.09	0.22

Note: Only parameters that contribute more than one percent to the uncertainty are shown in the table. They explains 82% of uncertainty in the predicted population density.

Table S10 Uncertainty contributions (%) by different model parameters for the predicted population density of parous female adults at the community level

Parameters	Descriptions	Uncertainty contribution	Standard error
A-FS	Nominal daily survival rate for female adults	69.82	3.88
A-MS	Nominal daily survival rate for male adults	6.16	0.60
L-S	Nominal daily survival rate for larvae	3.51	0.42
Fd1	Coefficient of metabolic weight loss for larvae	2.85	0.38
L-D	Larval development rate	1.48	0.26
P-S	Nominal daily survival rate for pupae	1.00	0.21

Note: Only parameters that contribute more than one percent to the uncertainty are shown in the table. They explains 84.8% of uncertainty in the predicted population density.

Table S11 Uncertainty contributions (%) by different model parameters for the predicted population density of male adults at the community level

Parameters	Descriptions	Uncertainty contribution	Standard error
A-MS	Nominal daily survival rate for male adults	29.09	1.38
A-FS	Nominal daily survival rate for female adults	18.32	1.02
Fd1	Coefficient of metabolic weight loss for larvae	13.51	0.85
L-S	Nominal daily survival rate for larvae	10.82	0.74
L-D	Larval development rate	4.29	0.44
P-S	Nominal daily survival rate for pupae	4.27	0.44
E-PTH	High temperature limit for predator activities on eggs	3.11	0.36
P-SEM	Emergence probability for pupae	2.14	0.31
Fa	Conversion rate of consumed food to biomass for larvae	1.79	0.28
Fc	Coefficient of food dependence for larvae	1.06	0.21

Note: Only parameters that contribute more than one percent to the uncertainty are shown in the table. They explains 88.4% of uncertainty in the predicted population density.